AWARD NUMBER: **W81XWH-13-1-0247**

TITLE: **ENZYME-CATALYZED MUTATION IN BREAST CANCER**

PRINCIPAL INVESTIGATOR: **REUBEN S. HARRIS**

CONTRACTING ORGANIZATION: **UNIVERSITY OF MINNESOTA – TWIN CITIES**
**Minneapolis, MN 55455-2070**

REPORT DATE: **October 2015**

TYPE OF REPORT: **FINAL**

PREPARED FOR: U.S. Army Medical Research and Materiel Command
Fort Detrick, Maryland 21702-5012

# REPORT DOCUMENTATION PAGE

*Form Approved*
*OMB No. 0704-0188*



| 1. REPORT DATE | 2. REPORT TYPE | 3. DATES COVERED |
|---|---|---|
| October 2015 | Final | 1Aug2013 - 31Jul2015 |

**4. TITLE AND SUBTITLE**

ENZYME-CATALYZED MUTATION IN BREAST CANCER

**5a. CONTRACT NUMBER**

**5b. GRANT NUMBER**

W81XWH- 13-1-0247

**5c. PROGRAM ELEMENT NUMBER**

**6. AUTHOR(S)**

REUBEN S. HARRIS

E-Mail: rsh@umn.edu

**5d. PROJECT NUMBER**

**5e. TASK NUMBER**

**5f. WORK UNIT NUMBER**

**7. PERFORMING ORGANIZATION NAME(S) AND ADDRESS(ES)**

UNIVERSITY OF MINNESOTA – TWIN CITIES
Minneapolis, MN 55455-2070

**8. PERFORMING ORGANIZATION REPORT NUMBER**

**9. SPONSORING / MONITORING AGENCY NAME(S) AND ADDRESS(ES)**

U.S. Army Medical Research and Materiel Command
Fort Detrick, Maryland 21702-5012

**10. SPONSOR/MONITOR'S ACRONYM(S)**

**11. SPONSOR/MONITOR'S REPORT NUMBER(S)**

**12. DISTRIBUTION / AVAILABILITY STATEMENT**

Approved for Public Release; Distribution Unlimited

**13. SUPPLEMENTARY NOTES**

**14. ABSTRACT**

**The development of breast cancer, including late stage events such as metastasis and drug resistance, requires mutations. The origins of most of these mutations are unknown. We recently implicated the DNA cytosine deaminase APOBEC3B. This Idea Award studies tests the hypothesis that APOBEC3B causes a genome wide hypermutable state and the hypothesis that APOBEC3B alters the epigenome by cytosine deamination and methyl-cytosine deamination mechanisms, respectively. Positive results will be significant because they will delineate a major source of mutations and epigenetic changes in breast cancer, and thereby pave the way for new diagnostic/prognostic tests and methods to treat breast cancer by preventing the activity of this enzyme.**

**15. SUBJECT TERMS**

Nothing listed

| 16. SECURITY CLASSIFICATION OF: | | | 17. LIMITATION OF ABSTRACT | 18. NUMBER OF PAGES | 19a. NAME OF RESPONSIBLE PERSON |
|---|---|---|---|---|---|
| a. REPORT | b. ABSTRACT | c. THIS PAGE | | | USAMRMC |
| Unclassified | Unclassified | Unclassified | Unclassified | 47 | 19b. TELEPHONE NUMBER *(include area code)* |

**Table of Contents** **Page 2**

## Introduction

The development of breast cancer, including late stage events such as metastasis and drug resistance, requires mutations. The origins of most of these mutations are unknown. We recently implicated the DNA cytosine deaminase APOBEC3B. This Idea Award studies tests the hypothesis that APOBEC3B causes a genome wide hypermutable state and the hypothesis that APOBEC3B alters the epigenome by cytosine deamination and methyl-cytosine deamination mechanisms, respectively. Positive results will be significant because they will delineate a major source of mutations and epigenetic changes in breast cancer, and thereby pave the way for new diagnostic/prognostic tests and methods to treat breast cancer by preventing the activity of this enzyme.

**Keywords**

APOBEC3B; Apolipoprotein B mRNA editing enzyme, catalytic polypeptide-like-3 B; sometimes abbreviated A3B; one of 7 human A3 family members

C; Cytosine (a DNA and RNA base)

DNA; Deoxyribonucleic acid

ER; estrogen receptor (molecular target of the breast cancer therapeutic tamoxifen)

G; Guanine (a DNA and RNA base)

MeC; 5-methyl-cytosine (a common epigenetic modification in human DNA)

qPCR; Quantitative polymerase chain reaction

shRNA; short hairpin RNA (a molecular tool used to decrease gene expression)

SOW; Statement of Work

T; Thymine (a base typically found in DNA, but also the product of APOBEC3B-catalyzed MeC deamination)

U; Uracil (a base typically found in RNA but also the product of APOBEC3B-catalyzed C deamination)

**Overall Project Summary (significant revisions and/or additions to the original final report are highlighted in yellow)**

This section provides a final report and a narrative of progress over the 2 year duration of this Idea award. Please see **Table 1** below for an updated SOW including final reports of the status of each task. A summary and discussion (as requested) of the progress on each aim follows.

***Aim 1 – Does A3B cause a genome-wide hypermutable state?***

*Aim 1 rationale:* Although we have demonstrated APOBEC3B up-regulation in tumors and APOBEC3B activity in the nuclear extracts of several breast cancer cell lines[1], we still need to overcome the highest hurdle and demonstrate that APOBEC3B actually alters the genetic landscape of a breast cancer cell. This will be done by deep-sequencing to document the APOBEC3B-dependent contribution to the overall mutation distribution in cell lines and by performing a series of experiments with a well-established xenograft tumor model.

***Aim 1 - Summary of Results, Progress and Accomplishments with Discussion.***

*Aim 1A – deep-sequencing cell lines:* We have now deep sequenced several different cancer cell lines, and have encountered significant genetic heterogeneity in most instances that precluded analyses of APOBEC3B mutations. However, we have succeeded in one system in which APOBEC3B can be expressed inducibly. These results are detailed in **Appendix A**, an open access publication by **Akre *et al*., 2016, *PLoS One* (PMID: 27163364 PMCID: PMC4862684)** and discussed here.

Figure 1 shows doxycycline-induced expression of APOBEC3B. Figure 2 shows a titration of doxycycline levels that induce APOBEC3B expression and result in approximately 90% cell death. This level of doxycycline was used to induce 10-rounds of APOBEC3B expression and mutagenesis in daughter pools. Representative cells were then outgrown from each pool (single cell cloned) and subjected to microarray analysis for single nucleotide polymorphisms (SNPs) and full genome DNA sequencing. Figure 3 shows the results of the microarray analysis with increased numbers of SNPs and increased levels of copy number variations (CNVs). Figure 4 shows the results of the full genome sequence analysis. As anticipated, APOBEC3B mutations were detected throughout the genome at elevated frequencies. However, unexpectedly, we discovered that this cell line is defective in mismatch repair and had very high background levels of mutation, which precluded more extensive analyses of the APOBEC3B mutational landscape. Nevertheless, this series of experiments demonstrated the genome-wide impact of APOBEC3B and provided several valuable lessons to apply in future studies.

*Aim 1B – xenograft experiments in mice:* The proposed xenograft studies took longer than expected in part due to repeating key experiments and due to adding an over-expression study. However, we are delighted to report that the results are positive, and that therapy (tamoxifen) resistance in the ER+ breast cancer cell line MCF-7L is dependent upon APOBEC3B. Specifically, APOBEC3B knockdown slows down the rate of tumor evolution and drug resistance, and APOBEC3B over-expression speeds-up tumor

evolution and drug resistance. These analyses, included extensive methodologies, are detailed in **Appendix B**, an open access publication by **Law *et al*., 2016, *Science Advances* (PMID: 27730215 PMCID: PMC5055383)** and discussed here.

Figure 1 reports clinical data from our Dutch collaborators. A significant correlation is evident between APOBEC3B mRNA levels in primary tumors and progression free survival upon disease recurrence. Essentially, the higher the APOBEC3B levels in the original tumor, the poorer the outcomes in the recurrent setting for ER+ disease subjected to tamoxifen monotherapy. Figure 2 shows that shRNA mediated knockdown of APOBEC3B in the ER+ breast cancer cell line MCF-7L is robust and, importantly, that it does not alter cellular growth rates in culture. Figure 3 is a representative xenograft experiment in which APOBEC3B knockdown improves the durability of tamoxifen treatment by reducing the rate of developing drug resistance. Figures 4 and 5 show the results of APOBEC3B overexpression using a novel lentivirus-based construct (schematic in Figure 4A). Importantly, overexpression of the wildtype APOBEC3B enzyme, but not a catalytically dead form, reduces the durability of tamoxifen treatment by accelerating the rate of developing drug resistance. Taken together, these results are the first to demonstrate that altering the cellular levels of a single enzyme, APOBEC3B, can systematically influence the rate of acquired resistance to tamoxifen therapy.

Although this study was successful, it also faced some technical challenges. For instance, the MCF-7L cell line is genetically heterogeneous, which precluded the identification of the resistance mutations by exome sequencing. However, we have learned from these challenges and have taken a number of precautions, including the utilization of pre-defined clonogenic breast cancer cell lines, that we are confident will enable future successes.

***Aim 2 – Does A3B impact genomic MeC levels?***

*Aim 2 rationale:* The impetus for this aim stems from observations that the related DNA deaminases AID and APOBEC3A elicit MeC-to-T editing activity *in vitro*[2-4], and AID has been implicated in altering the MeC status of mouse germ and stem cells[5, 6]. Since AID is not expressed in normal breast epithelium or breast tumor cells and only A3B is up-regulated in breast tumors[1], we hypothesize that A3B alone has the capacity to remodel the breast cancer MeC landscape. This hypothesis will be tested here in experiments that are complementary to those described above.

***Aim 2 - Summary of Results, Progress and Accomplishments with Discussion.***

*Aims 2A-C:* We have completed the original studies as proposed and have found that APOBEC3B is not likely to have a role in genomic DNA demethylation (although it can do so biochemically). In essence, bisulfite sequencing has not identified any sites in the genome that become hypomethylated in APOBEC3B over-expressing cell lines in comparison to non-APOBEC3B expressing controls. We are concerned that the developmental fate of cell lines is difficult to alter, and that future studies in mice *in vivo* may be more informative.

| **Table 1. Progress on original SOW with current status/progress highlighted in blue.** | | |
|---|---|---|
| **Aim 1: Does APOBEC3B cause a genome-wide hypermutable state?** | | |
| **Task** | **Methods employed** | **Timeline and Status** |
| Engineering breast cancer cell lines MDA-MB-231, MDA-MB-453, MDA-MB-468, and HCC1569 to knock-down endogenous A3B and generate control lines; generate multiple sub-clones for each line. | Molecular biology, cell culture, qRT-PCR | Months 1-6; completed as proposed |
| Preparation of genomic DNA from selected cell lines (likely HCC1569) prepared in the above tasks to express high or low levels of A3B. Delivery of DNA to sequencing facility for whole exome capture, deep sequencing, and data/sequence analysis. | General molecular biology techniques, data/sequence analysis, bioinformatics | Months 6-18; sequencing done but results ambiguous because most cell lines were heterogenous; we have had success with one cell line and the results were published in *PLoS One* (**Appendix A – Akre *et al.*, 2016**). |
| Completion of IACUC forms for approval of animal experiments (80 NCr nude mice are proposed for the full xenograft experiment with numbers determined by power analysis – details can be found in the main text of the proposal). Once approved, the engineered cell lines described above (and in the narrative) will begin being xenografted into mice and therapies administered. | Cell culture, mouse model techniques | Months 1-5 for IACUC review, months 6-18 for animal procurement and xenograft experiments; IACUC approval was received, the cell lines were engineered, and the xenograft experiments were done |
| Tumor collection and analysis from xenografts. | Mouse model techniques, cancer-molecular biology techniques, qRT-PCR, sequence analysis | Months 16-20; done but DNA sequencing results were ambiguous because the cell line was |

| | | |
|---|---|---|
| | | heterogenous |
| Prepare data for publication. Publish manuscript. | Data analysis and writing | Months 20-24; a manuscript has been published in *Science Advances* (**Appendix B – Law *et al.*, 2016**). |
| | | |
| **Aim 2: Does APOBEC3B impact the genomic methyl-cytosine landscape?** | | |
| **Task** | **Methods** | **Timeframe** |
| Engineering of cell lines MDA-MB-231, MDA-MB-453, MDA-MB-468, and HCC1569 to knock-down endogenous A3B. Passage of lines from generations 2-32, with collection of DNA at generations 2, 4, 8, 16, and 32. Assessment of MeC levels using MeC ELISA kit. | Cell culture, molecular biology techniques, western blotting, qRT-PCR, ELISA | Months 1-6; completed as proposed. |
| In parallel with the task immediately above, the same DNA samples will be assessed for MeC content using HPLC-MS/MS, rather than ELISA. | Cell culture, molecular biology techniques, western blotting, qRT-PCR, HPLC-MS/MS | Months 2-7; completed as proposed. |
| Again, the same DNA samples as in the previous 2 tasks will be subjected to bisulfite sequencing to assess DNA methylation status in regions of the genome that are known to be effected by hypomethylation (see narrative for further details). | Cell culture, molecular biology techniques, deep-sequencing western blotting, qRT-PCR, bisulfite sequencing | Months 3-12; completed but the bisulfite DNA sequencing results were ambiguous because the cell line was heterogenous |
| We will engineer the non-tumorigenic cell lines MCF-10A (previously acquired from ATCC) and hTERT-HMEC (a gift from the lab of Dr. Vitaly Polunovsky) to over-express A3B by transfection with a linearized, tagged A3B-espression cassette followed by selection of stable clones. Control lines will be generated using the catalytically dead, tagged A3B-E255Q. | Cell culture, molecular biology techniques, western blotting, qRT-PCR | Months 3-12; completed as proposed. |
| Assessment of A3B over-expressing engineered cell lines' ability to alter the levels of MeC in the cell genome (determined by ELISA, HPLC-MS/MS, and bisulfite-sequencing). | Cell culture, cancer-molecular biology techniques, ELISA, HPLC-MS/MS, bisulfite sequencing | Months 8-16; completed as proposed. |
| Bisulfite-coupled deep sequencing will be performed to | Bisulfite-coupled | Months 15-22; |

| | | |
|---|---|---|
| quantify the levels of demethylation and identify any demethylation hot-spots and mutational spectra as a function of A3B expression. Samples sent for sequencing will be pairs of A3B high/A3B knock-down and A3B over-expressed/A3B-E255Q over-expressed DNA determined empirically from the previous aims to have positive results by ELISA, HPLC-MS/MS, and local bisulfite sequencing. | deep sequencing | completed but the bisulfite DNA sequencing results were ambiguous because the cell line was heterogenous |
| Analysis and compilation of data. Assembly of manuscript. | Data analysis and writing | Months 20-24; we have invested almost all effort in the success of Aim 1 once we learned Aim 2 would test negative. |

**Key Research Accomplishments**

1) Cell lines have been constructed that inducibly express APOBEC3B, and demonstrate the genome-wide nature of this breast cancer mutagenesis mechanism **[Appendix A: Akre *et al*., 2016, *PLoS One* (PMID: 27163364 PMCID: PMC4862684)]**.

2) Xenograft experiments with the ER+ breast cancer cell line MCF7L have demonstrated that APOBEC3B is a significant driver of tumor evolution and resistance to the SERM tamoxifen **[Appendix B: Law *et al*., 2016, *Science Advances* (PMID: 27730215 PMCID: PMC5055383)].**

## Conclusion

We are thrilled to report that our xenograft studies have been successful, and allowed us to demonstrate that APOBEC3B drives tamoxifen resistance in an ER+ breast cancer cell line (Law *et al*., 2016, *Science Advances*). Due to the fundamental nature of the underlying mutational process and the breadth of APOBEC3B over-expression in breast and other cancer types, this result is likely to be broadly applicable. The next step will be developing strategies to stop APOBEC3B driven breast tumor evolution in the hope of improving the efficacy of existing therapies such as tamoxifen, which can be undermined by tumor evolution and the acquisition of resistance mutations.

## Publications, Abstracts and Presentations

*Publications Acknowledging DoD Idea Award Support:*

Harris, R.S. (2013) Cancer mutation signatures, DNA damage mechanisms, and potential clinical implications. *Genome Medicine* 5:87 (3 pages). PMID: 24073723; PMCID: PMC3978439

Swanton, C., N. McGranahan, G.J. Starrett & R.S. Harris (2015) APOBEC enzymes: mutagenic fuel for cancer evolution and heterogeneity. *Cancer Discovery* 5:704-12. PMID: 26091828; PMCID: PMC4497973

Harris, R.S. (2015) Molecular mechanism and clinical impact of APOBEC3B-catalyzed mutagenesis in breast cancer. *Breast Cancer Research* 17:8 (10 pages). PMID: 25778352; PMCID: PMC4303225

**Appendix A:** Akre*, M.K, G.J. Starrett*, J.S. Quist, N.A. Temiz, M.A. Carpenter, A.N.J. Tutt, A. Grigoriadis & R.S. Harris (2016) Mutation processes in 293-based clones overexpressing the DNA cytosine deaminase APOBEC3B. *PLoS One* 11(5):e0155391. doi: 10.1371/journal.pone.0155391 (*equal contributions). PMID: 27163364; PMCID: PMC4862684

**Appendix B:** Law*, E.K., A.M. Sieuwerts*, K. LaPara, B. Leonard, G.J. Starrett, A.M. Molan, N.A. Temiz, R. Isaksson Vogel, M.E. Meijer-van Gelder, F.C.G.J. Sweep, P.N. Span, J.A. Foekens, J.W.M. Martens, D. Yee & R.S. Harris (2016) The DNA cytosine deaminase APOBEC3B promotes tamoxifen resistance in ER+ breast cancer. *Science Advances* 2, e1601737 (9 pages; *equal contributions). PMID: 27730215; PMCID: PMC5055383

*Oral Presentations Acknowledging DoD Idea Award Support:*

R.S. Harris; 8/13; "Evidence for APOBEC3B mutagenesis in multiple human cancers", Center for Molecular Medicine Norway, Oslo (Hans Prydz Distinguished Guest Lecture invited by Dr. H. Nilsen)

R.S. Harris; 10/13; "Integral roles for enzymatic DNA cytosine deamination in both antiviral innate immunity and cancer mutagenesis" University of Alberta, Edmonton, Canada (seminar invited by Dr. A. Mason)

R.S. Harris; 10/13; "Molecular and clinical impact of APOBEC3B mutagenesis in breast cancer", AACR special conference on Advances in Breast Cancer Research, San Diego, CA (talk invited by organizers)

R.S. Harris; 11/13; "Carcinogenesis fueled by enzyme-catalyzed DNA cytosine deamination", University of Virginia (talk invited by Drs. L. Hammarskjöld and D. Rekosh)

R.S. Harris; 11/13; "APOBEC3B mutagenesis in cancer", 29th Radiation Biology Center Symposium entitled: "Next generation radiation biology and beyond: New

perspectives on DNA damage and repair", Kyoto, Japan (talk invited by organizers)

R.S. Harris; 11/13; "APOBEC3 proteins in antiviral immunity and carcinogenesis", Kyoto University, Kyoto, Japan (talk invited by Dr. A. Takori-Kondo)

R.S. Harris; 2/14; "APOBEC3B-catalyzed mutagenesis in human cancer", NCI Frederick (talk invited by Dr. S. LeGrice)

R.S. Harris; 2/14; "APOBEC3 DNA deaminases in retrovirus restriction and cancer mutagenesis", University of Wisconsin at Madison (talk invited by Dr. D. Evans)

R.S. Harris; 4/14; "Mechanism and impact of enzymatic DNA cytosine deamination in human cancers", Wake Forest School of Medicine, Department of Biochemistry (talk invited by Dr. F. Perrino)

R.S. Harris; 7/14; "Can mutagenesis be a biomarker and a therapeutic target?", Stratified Medicine Symposium, UK NHS, Guy's Hospital, London, England (talk invited by Dr. Andrew Tutt and the organizing committee)

R.S. Harris; 9/14; "APOBEC3B mutagenesis in human cancer: basic mechanisms and clinical implications" AbCam Conference on Chromothripsis, Clustered Mutation and Complex Chromosome Rearrangements, Boston, MA (talk invited by Drs. Ralph Scully and James Haber)

R.S. Harris; 9/14; "APOBEC-mediated mutagenesis of viral and cancer genomes", IRCM, Montreal, Canada (talk invited by Dr. Javier DiNoia)

R.S. Harris; 9/14; "DNA editing in cancer" NCI workshop on RNA Editing, Epitranscriptomics, and Processing in Cancer Progression, Bethesda, MD (keynote talk invited by Drs. John Coffin and Betsy Read-Cannole)

R.S. Harris; 9/14; "The biological and pathological importance of enzyme-catalyzed DNA cytosine deamination", Innovative Approaches for Identification of Antiviral Agents Summer School (IAAASS), Sardinia, Italy (lecture invited by the organizing committee)

R.S. Harris; 10/14; "Cancer mutagenesis by the antiviral enzyme APOBEC3B" Genentech, San Francisco, CA (talk invited by Dr. Tim Behrens)

R.S. Harris; 10/14; "APOBEC3B mutagenesis in human cancer: basic mechanisms and clinical implications", Erasmus Medical Center, Holland (talk invited by Dr. John Martens)

R.S. Harris; 11/14; "APOBEC3 proteins, DNA uracil, and cancer mutagenesis" US-EU conference on repair of endogenous DNA damage, Santa Fe, NM (talk invited by the organizers)

R.S. Harris; 11/14; "APOBEC3B mutagenesis in human cancer: basic mechanisms and clinical implications", 10$^{th}$ National Cancer Research Institute Conference, BT Convention Center, Liverpool, UK (plenary talk invited by the organizing committee)

R.S. Harris; 12/14; "APOBEC3B mutagenesis in cancer: basic mechanisms and clinical implications" San Antonio Breast Cancer Symposium, San Antonio, TX (talk invited by the organizers)

R.S. Harris; 2/15; "Cancer mutagenesis by the antiviral DNA cytosine deaminase APOBEC3B", Mayo Clinic, Rochester, MN (talk invited by Dr. Yasuhiro Ikeda)

R.S. Harris; 2/15; "Virus restriction and cancer mutation by the APOBEC family of DNA cytosine deaminases ", Massey University, New Zealand (talk invited Dr. Elena Harjes)

R.S. Harris; 3/15; "DNA deamination in cancer mutagenesis", Gordon Research Conference on RNA Editing, Lucca (Barga), Italy (talk invited by the organizing committee)

R.S. Harris; 4/15; "Mechanism and clinical impact of APOBEC3B mutagenesis in cancer", Ohio State University, Columbus, OH (seminar invited by Dr. Kay Huebner)

R.S. Harris; 5/15; "APOBEC mutation signatures and the origins of mutation in breast cancer", IMPAKT, Brussels, Belgium (talk invited by the organizing committee)

R.S. Harris; 6/15; "Molecular mechanism and clinical impact of APOBEC mutagenesis in cancer", Istituto Superiore di Sanità (ISS), Rome, Italy (talk invited by Drs. Margherita Bignami and Eugenia Dogliotti)

R.S. Harris; 6/15; "Cancer mutagenesis by enzymatic DNA cytosine deamination", Ospedale Pediatrico Bambino Gesù, Rome, Italy (talk invited by Dr. Angela Gallo)

R.S. Harris; 7/15; "Antiviral enzymes in cancer – molecular mechanism and clinical implications", University of Cagliari, Italy (talk invited by Drs. Elias Maccioni and Enzo Tramontano)

R.S. Harris; 10/15; "APOBEC-catalyzed mutagenesis in cancer", Wistar Institute, Philadelphia, PA (seminar invited by Drs. Kazuko Nishikura and Ashani Weeraratna)

R.S. Harris; 10/15; "Genomic DNA deamination in cancer", 17$^{th}$ Annual John Goldman Conference on Chronic Myeloid Leukemia: Biology and Therapy, Lisbon, Portugal (talk invited by meeting organizers)

R.S. Harris; 11/14; "Retrovirus restriction and cancer mutagenesis through enzymatic DNA cytosine deamination", University of Toronto, Canada (talk invited by Dr. Jeffrey Lee)

R.S. Harris; 12/15; "Tamoxifen resistance driven by the DNA cytosine deaminase APOBEC3B in recurrent estrogen receptor positive breast cancer" San Antonio Breast Cancer Symposium, San Antonio, TX (talk invited by the organizers)

## Inventions, Patents and Licenses

Nothing to report.

**Reportable Outcomes**

Nothing to report.

**Other Achievements**

One Ph.D. student, Ms. Monica Akre, is being supported by this award. She passed her written and oral preliminary exams and she helped to complete the proposed studies in Aim 1A (**Appendix A**).

## References

[1] Burns MB, Lackey L, Carpenter MA, Rathore A, Land AM, Leonard B, et al. APOBEC3B is an enzymatic source of mutation in breast cancer. Nature. 2013;494:366-70.

[2] Morgan HD, Dean W, Coker HA, Reik W, Petersen-Mahrt SK. Activation-induced cytidine deaminase deaminates 5-methylcytosine in DNA and is expressed in pluripotent tissues: implications for epigenetic reprogramming. J Biol Chem. 2004;279:52353-60.

[3] Bransteitter R, Pham P, Scharff MD, Goodman MF. Activation-induced cytidine deaminase deaminates deoxycytidine on single-stranded DNA but requires the action of RNase. Proc Natl Acad Sci U S A. 2003;100:4102-7.

[4] Wijesinghe P, Bhagwat AS. Efficient deamination of 5-methylcytosines in DNA by human APOBEC3A, but not by AID or APOBEC3G. Nucleic Acids Res. 2012;40:9206-17.

[5] Popp C, Dean W, Feng S, Cokus SJ, Andrews S, Pellegrini M, et al. Genome-wide erasure of DNA methylation in mouse primordial germ cells is affected by AID deficiency. Nature. 2010;463:1101-5.

[6] Bhutani N, Brady JJ, Damian M, Sacco A, Corbel SY, Blau HM. Reprogramming towards pluripotency requires AID-dependent DNA demethylation. Nature. 2010;463:1042-7.

## Appendices

**Appendix A:** Akre*, M.K, G.J. Starrett*, J.S. Quist, N.A. Temiz, M.A. Carpenter, A.N.J. Tutt, A. Grigoriadis & R.S. Harris (2016) Mutation processes in 293-based clones overexpressing the DNA cytosine deaminase APOBEC3B. *PLoS One* 11(5):e0155391. doi: 10.1371/journal.pone.0155391 (*equal contributions). PMID: 27163364; PMCID: PMC4862684

**Appendix B:** Law*, E.K., A.M. Sieuwerts*, K. LaPara, B. Leonard, G.J. Starrett, A.M. Molan, N.A. Temiz, R. Isaksson Vogel, M.E. Meijer-van Gelder, F.C.G.J. Sweep, P.N. Span, J.A. Foekens, J.W.M. Martens, D. Yee & R.S. Harris (2016) The DNA cytosine deaminase APOBEC3B promotes tamoxifen resistance in ER+ breast cancer. *Science Advances* 2, e1601737 (9 pages; *equal contributions). PMID: 27730215; PMCID: PMC5055383

PLOS ONE

RESEARCH ARTICLE

# Mutation Processes in 293-Based Clones Overexpressing the DNA Cytosine Deaminase APOBEC3B

**Monica K. Akre[1☯], Gabriel J. Starrett[1☯], Jelmar S. Quist[2], Nuri A. Temiz[1], Michael A. Carpenter[1], Andrew N. J. Tutt[2], Anita Grigoriadis[2], Reuben S. Harris[1,3]***

**1** Department of Biochemistry, Molecular Biology, and Biophysics, Institute for Molecular Virology, Masonic Cancer Center, University of Minnesota, Minneapolis, MN, United States of America, **2** Breast Cancer Now Research Unit, Research Oncology, Guy's Hospital, King's College London, London, United Kingdom, **3** Howard Hughes Medical Institute, University of Minnesota, Minneapolis, MN, United States of America

☯ These authors contributed equally to this work.
* rsh@umn.edu



OPEN ACCESS

**Citation:** Akre MK, Starrett GJ, Quist JS, Temiz NA, Carpenter MA, Tutt ANJ, et al. (2016) Mutation Processes in 293-Based Clones Overexpressing the DNA Cytosine Deaminase APOBEC3B. PLoS ONE 11(5): e0155391. doi:10.1371/journal.pone.0155391

**Editor:** Javier Marcelo Di Noia, Institut de Recherches Cliniques de Montréal (IRCM), CANADA

**Received:** February 26, 2016

**Accepted:** April 5, 2016

**Published:** May 10, 2016



**Data Availability Statement:** All raw sequences are available from NCBI SRA under project number, PRJNA312357. All SNP data sets have been deposited in the NCBI GEO database under accession code GSE78710.

**Funding:** Work in the Grigoriadis and Tutt laboratories is supported by Breakthrough Breast Cancer (recently merged with Breast Cancer Campaign forming Breast Cancer Now). JQ is on a PhD studentship in Translational Medicine from the NIHR Biomedical Research Centre at Guy's and St Thomas. Cancer studies in the Harris laboratory are supported by grants from the Department of Defense

## Abstract

Molecular, cellular, and clinical studies have combined to demonstrate a contribution from the DNA cytosine deaminase APOBEC3B (A3B) to the overall mutation load in breast, head/neck, lung, bladder, cervical, ovarian, and other cancer types. However, the complete landscape of mutations attributable to this enzyme has yet to be determined in a controlled human cell system. We report a conditional and isogenic system for A3B induction, genomic DNA deamination, and mutagenesis. Human 293-derived cells were engineered to express doxycycline-inducible A3B-eGFP or eGFP constructs. Cells were subjected to 10 rounds of A3B-eGFP exposure that each caused 80–90% cell death. Control pools were subjected to parallel rounds of non-toxic eGFP exposure, and dilutions were done each round to mimic A3B-eGFP induced population fluctuations. Targeted sequencing of portions of *TP53* and *MYC* demonstrated greater mutation accumulation in the A3B-eGFP exposed pools. Clones were generated and microarray analyses were used to identify those with the greatest number of SNP alterations for whole genome sequencing. A3B-eGFP exposed clones showed global increases in C-to-T transition mutations, enrichments for cytosine mutations within A3B-preferred trinucleotide motifs, and more copy number aberrations. Surprisingly, both control and A3B-eGFP clones also elicited strong mutator phenotypes characteristic of defective mismatch repair. Despite this additional mutational process, the 293-based system characterized here still yielded a genome-wide view of A3B-catalyzed mutagenesis in human cells and a system for additional studies on the compounded effects of simultaneous mutation mechanisms in cancer cells.

## Introduction

Cancer genome sequencing studies have defined approximately 30 distinct mutation signatures (reviewed by [1–4]). Some signatures are large-scale confirmations of established sources of

Breast Cancer Research Program (BC121347), the Jimmy V Foundation for Cancer Research, the Norwegian Centennial Chair Program, the Minnesota Partnership for Biotechnology and Medical Genomics, and the Randy Shaver Cancer Research and Community Fund. Salary support for GJS was provided by a National Science Foundation Graduate Research Fellowship (DGE 13488264). RSH is an Investigator of the Howard Hughes Medical Institute. The funders had no role in study design, data collection and analysis, decision to publish, or preparation of the manuscript.

**Competing Interests:** RSH is a co-founder of ApoGen Biotechnologies Inc. The other authors declare no competing financial interests. This does not alter the authors' adherence to PLOS ONE policies on sharing data and materials.

DNA damage that escaped repair or were repaired incorrectly. The largest is water-mediated deamination of methyl-cytosine bases, which manifest as C-to-T transitions in genomic 5'-CG motifs [5]. This process impacts almost all cancer types and accumulates as a function of age. Other well known examples include ultraviolet radiation, UV-A and UV-B, which crosslink adjacent pyrimidine bases and result in signature C-to-T transitions [6], and tobacco mutagens such as nitrosamine ketone (NNK), which metabolize into reactive forms that covalently bind guanine bases and result in signature G-to-T transversions [7]. These latter mutagenic processes are well known drivers of skin cancer and lung cancer, respectively, but also contribute to other tumor types. A lesser-known but still significant example of a mutagen is the dietary supplement aristolochic acid, which is derived from wild ginger and related plants and metabolized into reactive species that covalently bind adenine bases and cause A-to-T transversions [8, 9]. Aristolochic acid mutation signatures are evident in urothelial cell, hepatocellular, and bladder carcinomas. Other confirmed mutation sources include genetic defects in recombination repair (*BRCA1*, *BRCA2*, etc.), post-replication mismatch repair (*MSH2*, *MLH1*, etc.), and DNA replication proofreading function, which manifest as microhomology-mediated insertion/deletion mutations, repeat/microsatellite slippage mutations, and transversion mutation signatures, respectively [4, 5, 10].

The largest previously undefined mutation signature in cancer is C-to-T transitions and C-to-G transversions within 5'-TC dinucleotide motifs [5, 11, 12]. This mutation signature occurs throughout the genome, as well as less frequently in dense clusters called kataegis. This signature is ascribable to the enzymatic activity of members of the APOBEC family of DNA cytosine to uracil deaminases [5, 11–15]. Human cells encode up to 9 distinct APOBEC family members with demonstrated C-to-U editing activity, and 7/9 have been shown to prefer 5'-TC dinucleotide motifs in single-stranded DNA substrates: APOBEC1, APOBEC3A, APOBEC3B (A3B), APOBEC3C, APOBEC3D, APOBEC3F, and APOBEC3H. In contrast, AID and APOBEC3G prefer 5'RC and 5'CC, respectively (R = purine; reviewed by [16, 17]). The size and similarity of this protein family, as well as the formal possibility that another DNA damage source may be responsible for the same mutation signature [18], have made DNA sequencing data and informatics analyses open to multiple interpretations.

However, independent [13, 19] and subsequent [14, 15, 20–26] studies indicate that at least one DNA deaminase family member, A3B, has a significant role in causing these types of mutations in cancer. A3B localizes to the nucleus throughout the cell cycle except during mitosis when it appears excluded from chromatin [19]. A3B is upregulated in breast cancer cell lines and primary tumors at the mRNA, protein, and activity levels [13, 20, 27]. Endogenous A3B is the only detectable deaminase activity in nuclear extracts of many cancer cell lines representing a broad spectrum of cancer types (breast, head/neck, lung, ovarian, cervix, and bladder [13, 20, 27]). Endogenous A3B is required for elevated levels of steady state uracil and mutation frequencies in breast cancer cell lines [13]. Overexpressed A3B induces a potent DNA damage response characterized by gamma-H2AX and 53BP1 accumulation, multinuclear cell formation, and cell cycle deregulation [13, 21, 22]. A3B levels correlate with overall mutation loads in breast and head/neck tumors [13, 23]. The biochemical deamination preference of recombinant A3B, 5'TCR, is similar to the actual cytosine mutation pattern observed in breast, head/neck, lung, cervical, and bladder cancers [13, 14, 20]. Human papillomavirus (HPV) infection induces A3B expression in several human cell types, providing a link between viral infection and the observed strong APOBEC mutation signatures in cervical and some head/neck and bladder cancers [28–30]. The spectrum of oncogenic mutations in *PIK3CA* is biased toward signature A3B mutation targets in HPV-positive head/neck cancers [23]. Last but not least, high *A3B* levels correlate with poor outcomes for estrogen receptor-positive breast cancer patients [25, 26, 31].

Despite this extensive and rapidly growing volume of genomic, molecular, and clinical information on A3B in cancer, the association between A3B and APOBEC mutational signatures has so far only been correlative, and a mechanistic demonstration of this enzyme's activity on the human genome has yet to be determined. Here we report further development of a human 293 cell-based system for conditional expression of human A3B. The results reveal, for the first time in a human cell line, the genomic landscape of A3B induced mutagenesis.

## Materials and Methods

### Cell Lines

We previously reported T-REx-293 cells that conditionally express A3B [13]. However, the mother, daughter, and granddaughter lines described here are new in order to ensure a single cell origin and have all of the controls derived in parallel. T-REx-293 cells were cultured in high glucose DMEM (Hyclone) supplemented with 10% FBS and 0.5% Pen/Strep. Single cell derived mother lines, A and C, were obtained by limiting dilution in normal growth medium. These mother clones were transfected with linearized pcDNA5/TO-A3Bintron-eGFP (A3Bi-eGFP) or pcDNA5/TO-eGFP vectors [13, 32], selected with 200 μg/mL hygromycin, and screened as described in the main text to identify drug-resistant daughter clones capable of Dox-mediated induction of A3Bi-eGFP or eGFP, respectively. The encoded A3B enzyme is identical to "isoform a" in GenBank (NP_004891.4). GFP flow cytometry was done using a FACSCanto II instrument (BD Biosciences).

### Immunoblots

Whole cell lysates were prepared by suspending $1x10^6$ cells in 300μL 10x reducing sample buffer (125mM Tris pH 6.8, 40% Glycerol, 4%SDS, 5% 2-mercaptoethanol and 0.05% bromophenol blue). Soluble proteins were fractionated by 4% stacking and 12% resolving SDS PAGE, and transferred to PVDF membranes using a wet transfer BioRad apparatus. Membranes were blocked for 1 hr in 4% milk in PBS with 0.05% sodium azide. Primary antibody incubations, anti-GFP (JL8-BD Clontech) and anti-β-actin (Cell Signaling) were done in at a 1:1000 dilution in 4% milk diluted in PBST, and incubation conditions ranged from 4–8 degrees C for 2–16 hrs. Membranes were then washed 3 times for 5 minutes in PBST. Secondary antibody incubations, anti-mouse 680 (1:20000) and anti-rabbit 800 (1:20000), were done in 4% milk diluted in PBST with 0.01% SDS, and incubation conditions ranged from 4–8 degrees C for 2–16 hrs. The resulting membranes were washed 3 times for 5 minutes in PBST and imaged using Licor instrumentation (Odyssey).

### DNA Deaminase Activity Assays

This assay was adapted from published procedures [27, 33]. Whole-cell extracts were prepared from $1x10^6$ cells by sonication in 200μL HED buffer (25mM HEPES, 5mM EDTA, 10% glycerol, 1mM DTT, and one tablet protease inhibitor-Roche per 50mL HED buffer). Debris was removed by a 30 min maximum speed spin in a tabletop micro-centrifuge at 4 degrees C. The supernatant was then used in 20μL deamination reactions that contained the following: 1μL of 4pM fluorescently-labeled 43-mer oligo (5'-ATTATTATTATTCGAATGGATTTATTTATT TATTTATTTATTT-fluorescein) containing a single interior 5'-TC substrate, 9.25μL UDG (NEB), 0.25μL RNase, 2μL 10x UDG buffer (NEB), 16.5μL lysate. Reactions were incubated at 37 degrees C for 1h. 2μL 1M NaOH was added and reaction was heated to 95 degrees C in a thermocycler for 10 min. 22μL of 2x formamide loading buffer was added to each sample. 5μL of each reaction was fractionated on a 15% TBE Urea Gel and imaged using a SynergyMx plate reader (BioTek).

## Differential DNA Denaturation (3D) PCR Experiments

This assay was adapted from published procedures [13, 34]. Genomic DNA was extracted from samples using a PureGene protocol (Gentra) and quantified using Nanodrop instrumentation (ThermoFisher Scientific). 20 ng of genomic DNA was subjected to one round of normal high denaturation temperature PCR using Taq Polymerase (Denville) and primers for *MYC* (5'-ACGTTAGCTTCACCAACAGG and 3'TTCATCAAAAACATCATCATCCAG) or *TP53* (5'GAGCTGGAGCTTAGGCTCCAGAAAGGACAA and 3'TTCCTAGCACTGCCCAACAACACCAGC). 383 bp and 376 bp PCR products were purified and quantified using qPCR with nested primer sets and SYBR Green detection (Roche 480 LightCycler; 5'ACGAGGAGGAGAACTTCTACCAGCA and 3'TTCATCTGCGACCCGGACGACGAGA for *MYC* and 5'TTCTCTTTTCCTATCCTGAGTAGTGGTAA and 3'TTATGCCTCAGATTCACTTTTATCACCTTT for *TP53*). Equivalent amounts of each PCR product were then used for 3D-PCR using the same nested PCR primer sets. The resulting 291 and 235 bp products were fractionated by agarose gel electrophoresis, purified using QIAEX II (Qiagen), cloned into a pJet vector (Fermentas), and subjected to sequencing (GENEWIZ). Alignments and mutation calls were done with Sequencher (Gene Codes Corporation).

## SNP Array Based Mutational Analysis

Granddaughter clones were established by limiting dilution after the final pulse round. Genomic DNA was prepared from daughter and granddaughter clones using the Gentra PureGene kit (Qiagen, Valencia, CA), quantified by agarose gel staining with ethidium bromide and by NanoDrop measurements (Thermo Scientific, Wilmington, DE), and subjected to SNP array analyses by Source BioScience (Cambridge, UK) using the Human OmniExpress-24v1-0 BeadChip (Illumina, San Diego, CA). Raw data were pre-processed in GenomeStudio using the Genotyping Module (Illumina, San Siego, CA). Genotype clustering was performed using the *humanomniexpress_24v1-0_a* cluster file, whereby probes with a GenCall score below 0.15, indicating low genotyping reliability, were discarded. All samples passed quality control as assessed by call rates and frequencies. Genotypes for a total of 716,503 probes were used for further analyses.

By comparing the genotypes of the granddaughter clones to the pre-pulsed daughter clones, six classes of base substitutions could be determined (C-to-T, C-to-G, C-to-A, T-to-G, T-to-C, and T-to-A). For example, a C-to-T transition occurred if the C/C genotype of the mother clone changed to a C/T genotype in the granddaughter clone. Given the design of some microarray probes (i.e., some probes detect the Watson-strand rather than the Crick-strand), a change from a G/G in the mother clone to a G/A genotype in the granddaughter clone was also scored as a C-to-T transition.

Chromosomal abnormalities in the genomes of granddaughter clones were identified with Nexus Copy Number 7.5 software (BioDiscovery, Hawthorne, CA), using the matched mother clone as a reference. SNPRank segmentation was applied and the segmented copy number data were further processed with the Tumor Aberrations Prediction Suite (TAPS) to obtain allele-specific copy number profiles [35]. All analyses were performed using the R statistical environment (http://www.R-project.org). The number of copy number alterations in the A3B-eGFP pulsed clones were determined based on the difference between the segment copy number counts of the A3B-eGFP pulsed clones and the eGFP pulsed clones. Segments which the eGFP pulsed granddaughter clones were not identical or had CN of 0 were excluded. These were subsequently binned by copy number loss or gain. All SNP data sets have been deposited in the NCBI GEO database under accession code GSE78710.

### Whole Genome Sequencing (WGS)

Library preparation and sequencing was performed by the Beijing Genome Institute (BGI) on the Illumina X Ten platform to an average of 34.5 ± 2.8 fold coverage using purified DNA from Pulse 10 subclone extractions described in the SNP array based methods. Sequences were aligned to the hg19 reference genome using BWA. PCR duplicates were marked and removed with Picard-tools (Broad). Somatic mutation calling was conducted using mpileup (SamTools), VarScan2 (Washington University, MO)), and MuTect (Broad Institute, MA). Mutations detected by both VarScan2 and MuTect were kept as true somatic mutations. VarScan2 was run using procedures describe by de Bruin and coworkers [24]. MuTect was run using default parameters. Alignments from CG1 and CG2 were used as "normal" controls for CA1 and CA3, respectively. Alignment from AG3 was used as the as "normal" control for AA3. CG1 and CG2 were used as normals for each other in order to determine their somatic mutations. Somatic mutations that were called against multiple "normal" genomes were merged to increase detection rates by overcoming regions of poor sequence coverage unique to either "normal" genome. Variants occurring at an allele frequency greater than 0.5 or falling into repetitive regions or those with consistent mapping errors were removed as described [24]. Somatic indels were called by VarScan2 and filtered using the same methods described above. Separation of mutation signatures present in our WGS data was performed by the Somatic Signatures R package using nsNMF decomposition instead of Brunet NMF decomposition as described by Covington and colleagues [36]. Mutation strand asymmetries were analyzed using somatic mutations from all samples and the AsymTools MatLab software [37]. All raw sequences are available from NCBI SRA under project number, PRJNA312357.

## Results

### System for Conditional A3B Expression

Previous studies have demonstrated that A3B over-expression induces a strong DNA damage response resulting in cell cycle aberrations and eventual cell death [13, 19, 21, 22, 32]. To be able to control the degree of A3B-induced genotoxicity, we built upon our prior studies [13] by establishing a single cell-derived isogenic system for conditional and titratable expression of this enzyme. T-REx-293 cells were subcloned to establish an isogenic "mother" line, which was then transfected stably with a doxycycline (Dox) inducible A3B-eGFP construct or with an eGFP vector as a negative control. The resulting "daughter" clones were screened by flow cytometry to identify those that were non-fluorescent without Dox (i.e., non-leaky) and uniformly fluorescent with Dox treatment (**Fig 1A**). Daughter clones were also screened for Dox-inducible overexpression of A3B-eGFP or eGFP by anti-GFP immunoblotting (**Fig 1B**). A3B-eGFP clones were uniformly GFP-negative without Dox treatment, but eGFP only clones showed a low level of leaky expression possibly related to greater protein stability. As additional confirmation, the functionality of the induced A3B-eGFP protein was tested using an *in vitro* ssDNA deamination assay using whole cell extracts [33]. As expected, only extracts from Dox-treated A3B-eGFP cells elicited strong ssDNA C-to-U editing activity as evidenced by the accumulation of the deaminated and hydrolytically cleaved reaction products (labeled P in **Fig 1C**; see Methods for details). Nearly identical results were obtained with a parallel set of independently derived daughter clones (**Fig 1D and 1E**).

### Iterative Rounds of A3B Exposure

To establish reproducible A3B induction conditions, a series of cytotoxicity experiments was done using a range of Dox concentrations. 10,000 T-REx-293 A3B-eGFP cells were plated in 10 cm plates in triplicate, treated with 0, 1, 4, or 16 ng/mL Dox, incubated 14 days to allow

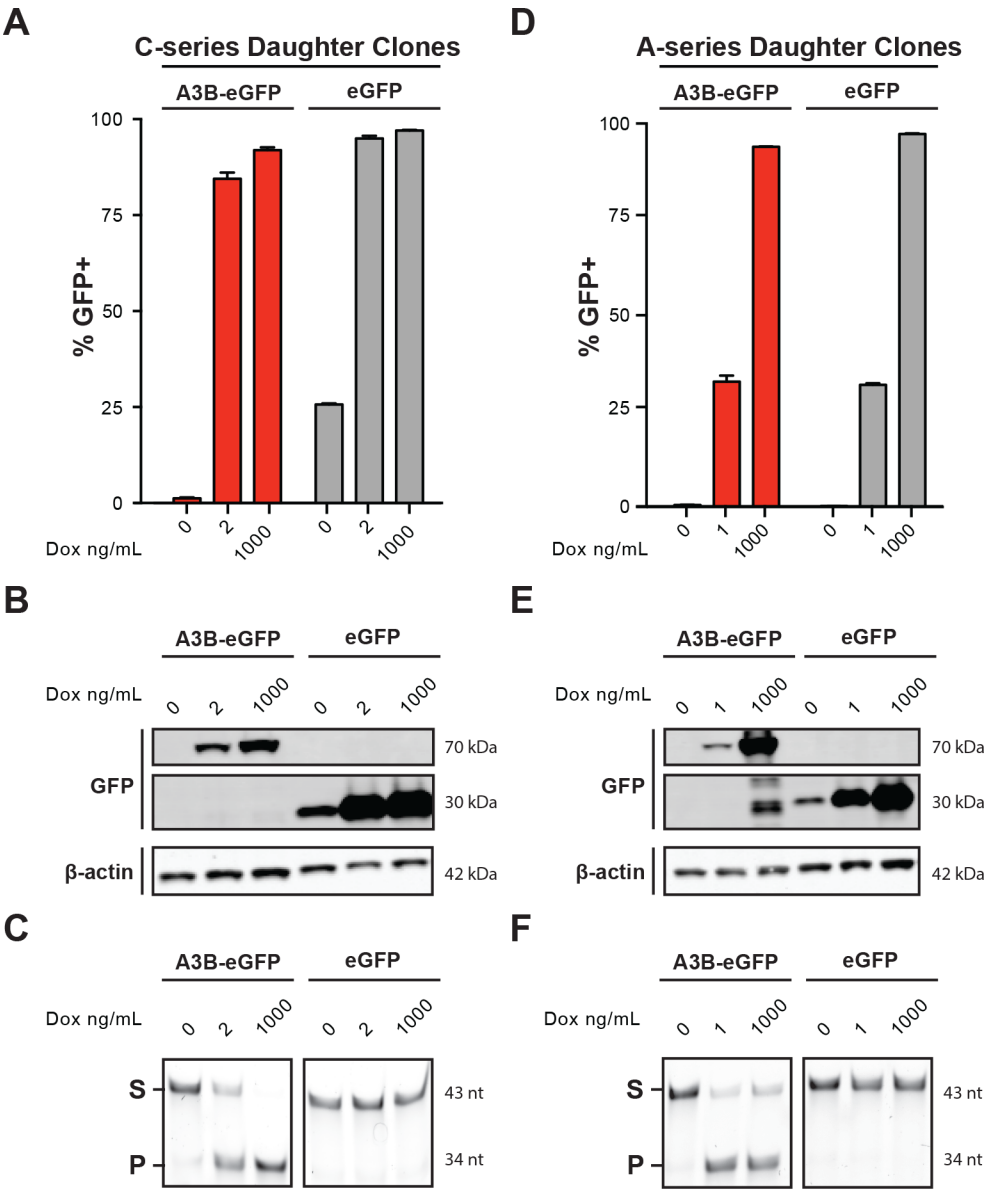


**Fig 1. A conditional system for A3B expression.** (A) Flow cytometry data for T-REx-293 A3B-eGFP and eGFP daughter cultures 24 hrs after Dox treatment (n = 3; mean +/- SD of technical replicates). (B) Anti-GFP immunoblot of T-REx-293 A3B-eGFP and eGFP daughter cultures 24 hrs after Dox treatment. (C) DNA cytosine deaminase activity data of whole cell extracts from T-REx-293 A3B-eGFP and eGFP daughter cultures 24 hrs after Dox treatment. (D, E, F) Biological replicate data using A-series daughter clones of the experiments described in panels A, B, and C, which used C-series daughter clones.

doi:10.1371/journal.pone.0155391.g001

time for colony formation, and quantified by crystal violet staining. As expected, higher Dox concentrations led to greater levels of toxicity (Fig 2A and 2B). Interpolation from a best-fit logarithmic curve indicated that 2 ng/mL Dox (C-series daughter clone) or 1 ng/mL Dox (A-series daughter clone) would cause 80–90% cytotoxicity, and this concentration was selected for subsequent experiments. Taken together with the measured doubling times of daughter clones, each A3B-eGFP induction series was estimated to span 7 days (represented in the work-flow schematic in Fig 2C).

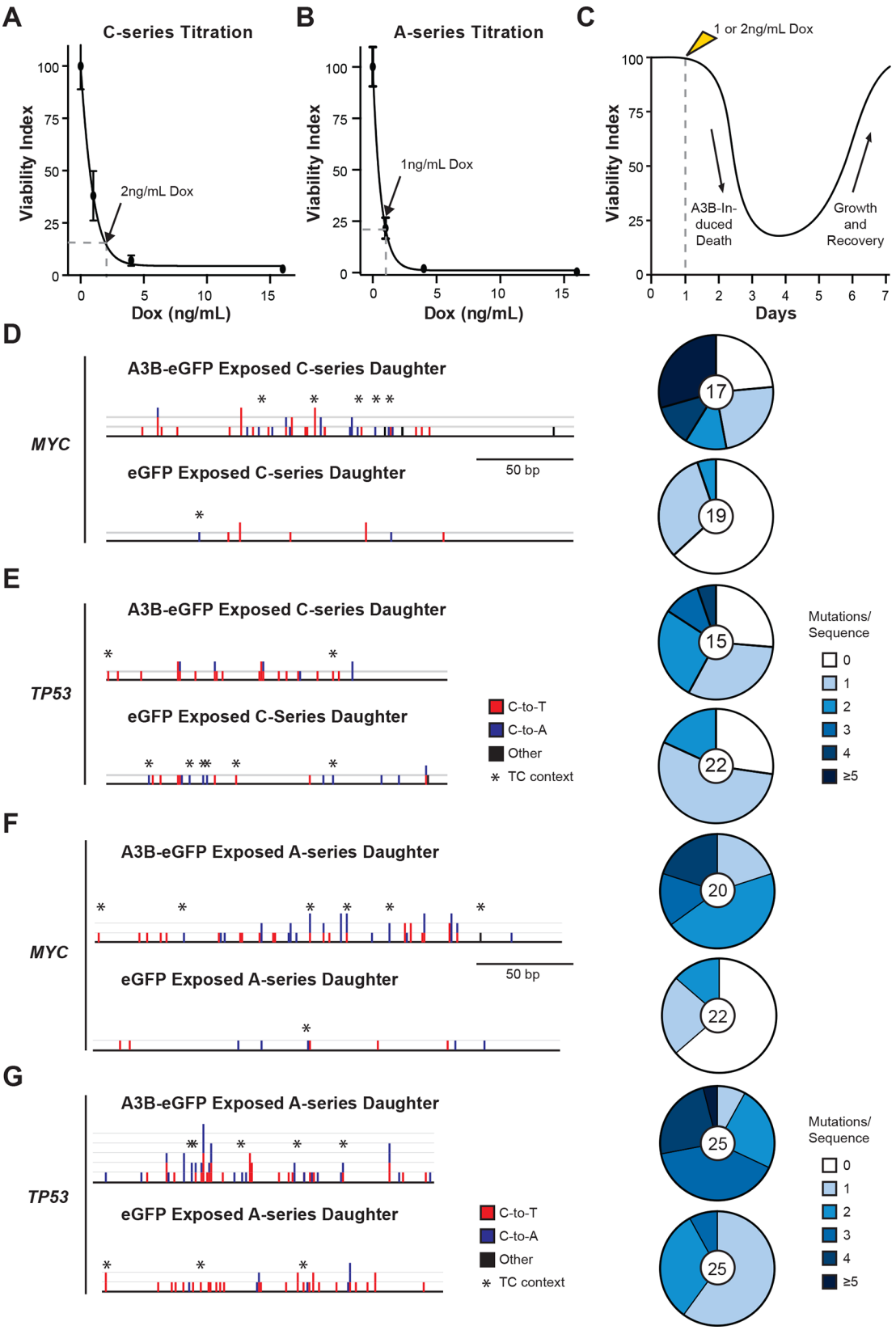
A
C-series Titration
Viability Index
100
75
50
25
0
2ng/mL Dox
0
5
10
15
Dox (ng/mL)
B
A-series Titration
Viability Index
1ng/mL Dox
Dox (ng/mL)
C
1 or 2ng/mL Dox
Viability Index
A3B-In-
duced
Death
Growth
and
Recovery
0
1
2
3
4
5
6
7
Days
D
A3B-eGFP Exposed C-series Daughter
MYC
50 bp
eGFP Exposed C-series Daughter
17
19
E
A3B-eGFP Exposed C-series Daughter
TP53
eGFP Exposed C-Series Daughter
C-to-T
C-to-A
Other
TC context
15
22
Mutations/
Sequence
0
1
2
3
4
≥5
F
A3B-eGFP Exposed A-series Daughter
MYC
50 bp
eGFP Exposed A-series Daughter
20
22
G
A3B-eGFP Exposed A-series Daughter
TP53
eGFP Exposed A-series Daughter
C-to-T
C-to-A
Other
TC context
25
25
Mutations/
Sequence
0
1
2
3
4
≥5

**Fig 2. A3B induction optimization and targeted sequencing results.** (A, B) Dose response curves indicating the relative colony forming efficiency (viability index) of T-REx-293 A3B-eGFP daughter clones treated with the indicated Dox concentrations (n = 3; mean viability +/- SD of biological replicates). The dotted lines show the Dox concentration required to induce 80% cell death (2 or 1 ng/mL for C- and A-series daughter clones, respectively). (C) A schematic representation of the experimental workflow depicting the viability index of a population of cells induced to express A3B-eGFP and recover over time. Dox treatment occurs on day 1, maximal death is observed on days 3 or 4, and each population typically rebounds to normal viability levels by days 6 or 7. (D-G) A summary of the base substitution mutations observed in *MYC* (241 bp) and *TP53* (176 bp) by 3D-PCR analysis of genomic DNA after 10 rounds of A3B-eGFP or eGFP exposure. Red, blue, and black columns represent the absolute numbers of C-to-T, C-to-A, and other base substitution types in sequenced 3D-PCR products, respectively. Asterisks indicate cytosine mutations occurring in 5'-TC dinucleotide motifs. The adjacent pie graphs summarize the base substitution mutation load for each 3D-PCR amplicon. The number of sequences analyzed is indicated in the center of each pie graph.

doi:10.1371/journal.pone.0155391.g002

Each T-REx-293 A3B-eGFP daughter clone was then subjected to 10 rounds of A3B-eGFP induction and recovery (Fig 2C). Iterative exposures to A3B-eGFP were expected to generate dispersed mutations throughout the genome. Ten rounds of A3B-eGFP induction were chosen as a sufficient regimen for the cells to accumulate readily detectable levels of somatic mutation as a proof-of-concept for this inducible system. This approach also left open the option to go back and characterize an intermediate round, or pursue additional rounds should analyses require less or more mutations, respectively.

A potential pitfall of this experimental approach is the possibility of selecting cells that have inactivated the A3B expression construct or the capacity for induction to avoid the cytotoxic effects of overexpressing this DNA deaminase. Aliquots of cells from each pulse series were therefore periodically tested by flow cytometry for A3B-eGFP inducibility, western blot for protein expression, and ssDNA deamination assays for enzymatic activity (e.g., Fig 1). Even after the tenth induction series, the A3B-eGFP daughter clones performed similar to original daughter cultures as well as to daughter cultures that had been grown continuously in parallel to the Dox-exposed experimental cultures and diluted to mimic the population dynamics caused by each A3B-eGFP exposure (e.g., Fig 1). These observations indicate that, despite negative selection pressure imposed by A3B-eGFP mediated DNA damage, resistance or escape mechanisms did not become overt.

## Targeted DNA Sequencing Provides Evidence for A3B Mutagenesis

Next, target gene 3D-PCR and sequencing were used to determine if the cells within each daughter culture had accumulated detectable levels of mutation after 10 rounds of A3B-eGFP exposure. 3D-PCR is a technique that enables the preferential recovery of DNA templates with C-to-T transitions and/or C-to-A transversions, because these mutations cause reduced hydrogen bonding potential and yield DNA molecules that can be amplified at PCR denaturation temperatures lower than those required to amplify the original non-mutated sequences [13, 38, 39]. *MYC* and *TP53* were selected as target genes for this analysis because our prior work with transiently over-expressed A3B and by others with related A3 family members has demonstrated that these genomic regions are susceptible to enzyme-catalyzed deamination [13, 34, 40–46].

The 3D-PCR and DNA sequencing analyses revealed substantially more mutations in *MYC* and *TP53* in A3B-eGFP exposed daughter cultures in comparison to controls (Fig 2D–2G). For instance, in the C-series daughter clone 43 mutations, mostly C-to-T transitions, were evident in *MYC* amplicons from A3B-eGFP exposed cultures, whereas only 9 mutations were found in a similar number of control amplicons (mutation plot on left side of Fig 2D; $p = 0.00036$, Student's two-tailed t-test). The mutation load per amplicon was also higher (pie graphs on right side of Fig 2D). Similar results were obtained for *TP53* (Fig 2E; $p = 0.11$, Student's two-tailed t-test), as well as for both *MYC* and *TP53* in a parallel set of independently

derived A-series daughter clones (Fig 2F and 2G; $p<0.0001$ and $p<0.0001$, respectively, Student's two-tailed t-test). The differences between A3B-eGFP exposed and control conditions were statistically significant for three of four conditions and, taken together, these results provided strong confirmation that 10 rounds of A3B-eGFP exposure caused increased levels of genomic DNA mutagenesis.

## Genome Wide Mutation Analyses

The experiments described used pools of cells and, due to the largely stochastic nature of the A3B mutational process and the duration of the pulse series, each pool would be expected to manifest extreme genetic heterogeneity. This complexity would constrain a standard deep sequencing approach by enabling only the earliest arising mutations to be detected in the pool because most subsequent mutations would persist at frequencies too low for reliable detection. To reduce this complexity to a manageable level and be able to investigate the mutational history of a single cell exposed to iterative rounds of either A3B-eGFP or eGFP, we used limiting dilution to generate "granddaughter" subclones from the tenth generation daughter pools. The strength of this strategy is that any new base substitution in a single daughter cell, which occurred between the time the daughter clone was originally generated until the recovery period following the tenth Dox treatment, would be fixed in the granddaughter clonal population at a predictable allele frequency depending on local chromosome ploidy (i.e., new mutations would be expected at 50% in diploid regions, 33% in triploid regions, 25% in tetraploid regions, etc., of the 293 cell genome).

The dynastic relationship between mother, daughter, and granddaughter clones in this study is shown in Fig 3A. To provide initial estimates of the overall level of new base substitution mutations, genomic DNA was extracted from each granddaughter clone and subjected to single nucleotide polymorphism (SNP) analysis using the Illumina OmniExpress Bead Chip. A base substitution mutation was defined as a clear SNP difference between each daughter clone and her respective granddaughter clone. These analyses revealed a wide range of SNP alterations among granddaughter clones, ranging from a low of <500 in the C-series eGFP expressing granddaughter subclone CG1 to a high of over 8,000 in the A-series A3B-eGFP expressing granddaughter subclone AA3 (Fig 3B). This extensive variability was expected based on the sublethal Dox concentration used in each exposure round, the randomness of granddaughter clone selection, and the stochastic nature of the mutation processes. Nevertheless, A3B-eGFP exposed granddaughter clones had an average of 3.4-fold more new cytosine mutations than the eGFP controls (averages shown by dashed vertical lines in Fig 3B). Sanger sequencing of cloned PCR products was used to confirm several distinct SNP alterations and provided an orthologous validation of this array-based approach (e.g., representative chromatograms of mutations in granddaughter CA1 versus corresponding non-mutated sequences from CG2 in Fig 3C). In addition, hundreds more genomic copy number alterations were evident in A3B-eGFP exposed granddaughters in comparison eGFP controls (Fig 3D). Interestingly, the overall number of copy number alterations appeared to correlate positively with the overall number of cytosine mutations, suggesting that many A3B-catalyzed genomic DNA deamination events are likely processed into DNA breaks and result in larger-scale copy number aberrations (Fig 3E).

## A3B Mutational Landscape by Whole Genome Sequencing

Next, whole genome sequencing (WGS) was done to assess the mutation landscape for 3 A3B-eGFP exposed and 3 eGFP control granddaughter clones from two distinct biological replica experiments (granddaughters depicted in Fig 3A). Samples were sequenced using the Illumina X Ten platform at the Beijing Genome Institute. Approximately 700 million 150 bp paired-end

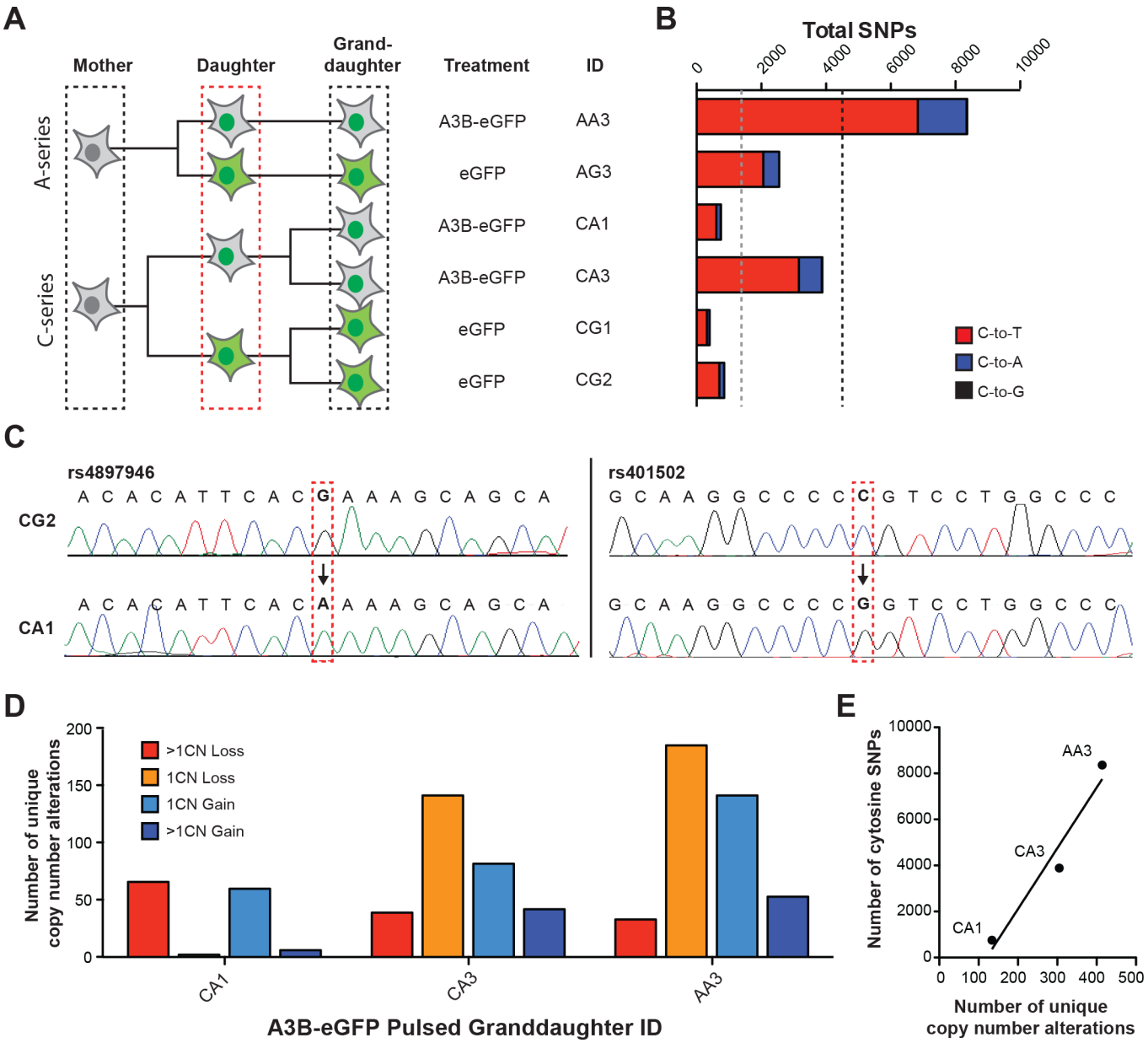


**Fig 3. SNP analyses to estimate new mutation accumulation.** (A) A dynastic tree illustrating the relationship between mother, daughter, and granddaughter clones used for SNP and WGS experiments. The red, dashed box around the daughter clones denotes 10 cycles of Dox-treatment. (B) A histogram summarizing the SNP alterations observed in granddaughter clones by microarray hybridization. Red, blue, and black colors represent C-to-T, C-to-A, and C-to-G mutations, respectively. (C) Sanger sequencing chromatograms confirming representative cytosine mutations predicted by SNP analysis. The left chromatogram shows a G-to-A transition (C-to-T on the opposite strand) and the right chromatogram a C-to-G transversion. (D) A histogram plot of the total number of copy number (CN) alterations in the indicated categories in A3B-eGFP exposed granddaughter clones in comparison to eGFP exposed controls, which were normalized to zero in order to make this comparison. (E) A dot plot and best-fit line of data in panel B versus data in panel D.

doi:10.1371/journal.pone.0155391.g003

reads were generated for each genome, with an average read depth of 34.5 ± 2.8 (SD) per locus. Reads were aligned against the hg19 genome with BWA and somatic mutations were called using both VarScan2 (Washington University, MO) and MuTect (Broad Institute, MA), with the intersection of the results these two methods identifying unambiguous mutations for further analysis [47, 48].

Using this conservative approach for mutation identification, a total of 6741, 3496, and 3530 somatic mutations occurred at cytosines in granddaughter clones that had been subjected to 10 rounds of A3B-eGFP pulses in comparison to only 910 and 1531 cytosine mutations in the eGFP controls, consistent with the results of the SNP analyses described above ($p = 0.018$, Student's t-test; **Fig 4A**; **S1 Table**). In particular, the A3B-eGFP pulsed granddaughter clones had higher proportions of C-to-T mutations than the eGFP controls, 59%, 54%, and 52% versus 36% and 47%, respectively (red slices in pie graphs in **Fig 4B**). The A3B-eGFP pulsed granddaughter clones also had higher proportions of mutations at A/T base pairs suggesting that genomic uracil lesions introduced by A3B may be processed by downstream error-prone repair processes analogous to those involved in AID-dependent somatic hypermutation of immunoglobulin genes [49] (**Fig 4A**).

However, despite finding significantly higher base substitution mutation loads in A3B-eGFP pulsed granddaughter clones, the overall distributions of cytosine mutations within the 16 possible trinucleotide contexts appeared visually similar for the A3B-eGFP and eGFP controls (histograms comparing the absolute frequencies of cytosine mutations with the 16 possible trinucleotide contexts are shown in **Fig 4C**). This result was initially surprising because we had expected obvious differences between the A3B-induced mutation spectrum and that attributable to other mechanisms, particularly within 5'TC contexts. However, a closer inspection of the eGFP control data sets strongly indicated that this 293-based system has a mutator phenotype possibly due to a defective replicative DNA polymerase proofreading domain and/or compromised post-replication mismatch repair [50, 51]. For instance, the eGFP controls had large numbers base substitution mutations (predominantly C-to-A, C-to-T, and T-to-C) as well as hallmark mutation asymmetries consistent with reported mutation spectra in mismatch repair defective tumors with microsatellite instabilities (**S1 Fig**) [5, 37, 51]. Moreover, each eGFP control had over 10,000 insertion/deletion mutations ranging in size from 1 to 46 base pairs (constrained by the length of the Illumina sequencing reads).

Therefore, to distinguish the A3B-eGFP induced mutation contribution from those caused by intrinsic sources, we used nsNMF decomposition via the Somatic Signatures R package to extract mutational signatures from granddaughter clones (**Methods**). This method extracted three signatures that explain 99.6% of the total variance in the observed mutation spectra. Extracted signature 1 (ES1) had large proportions of C-to-T mutations compared to the raw profiles observed for each sample. ES1 also contained low proportions of C-to-A mutations. The contribution of this signature to the overall mutation profile was specifically enriched in the A3B-eGFP pulsed granddaughter clones, contributing about 75% of all mutations (**Fig 4E**). Notably, this signature shows significant enrichments for C-to-T mutations within 5'TCG motifs, which are biochemically preferred by recombinant A3B enzyme [13, 14, 20] (Fisher's exact test for ES1 using the average of the total observed mutations across A3B-eGFP pulsed clones: TCA, $p = 0.17$; TCC, $p = 1.00$; TCG, $p < 0.0001$; TCT, $p = 0.017$). Moreover, strong enrichments for C-to-G transversion mutations were evident for cytosine mutations within TCW contexts (W = A or T) in ES1 in comparison to other trinucleotide combinations ($p = 0.0001$, Student's t-test). C-to-G transversions are hallmark A3B-mediated mutations because other known cytosine-biased mutational processes such as aging (spontaneous deamination of methyl-cytosines in 5'CG motifs) and UV-light (polymerase-mediated bypass of cross-linked pyrimidine bases) primarily result in C-to-T transitions [2, 52]. Extracted signatures 2 (ES2) and 3 (ES3) were characterized by large proportions of C-to-A mutations occurring independently of trinucleotide motif, in contrast to ES1. These WGS studies demonstrated increased genome-wide mutagenesis attributable to A3B, even over top of significant pre-existing mutation processes in this human 293 cell-based system.

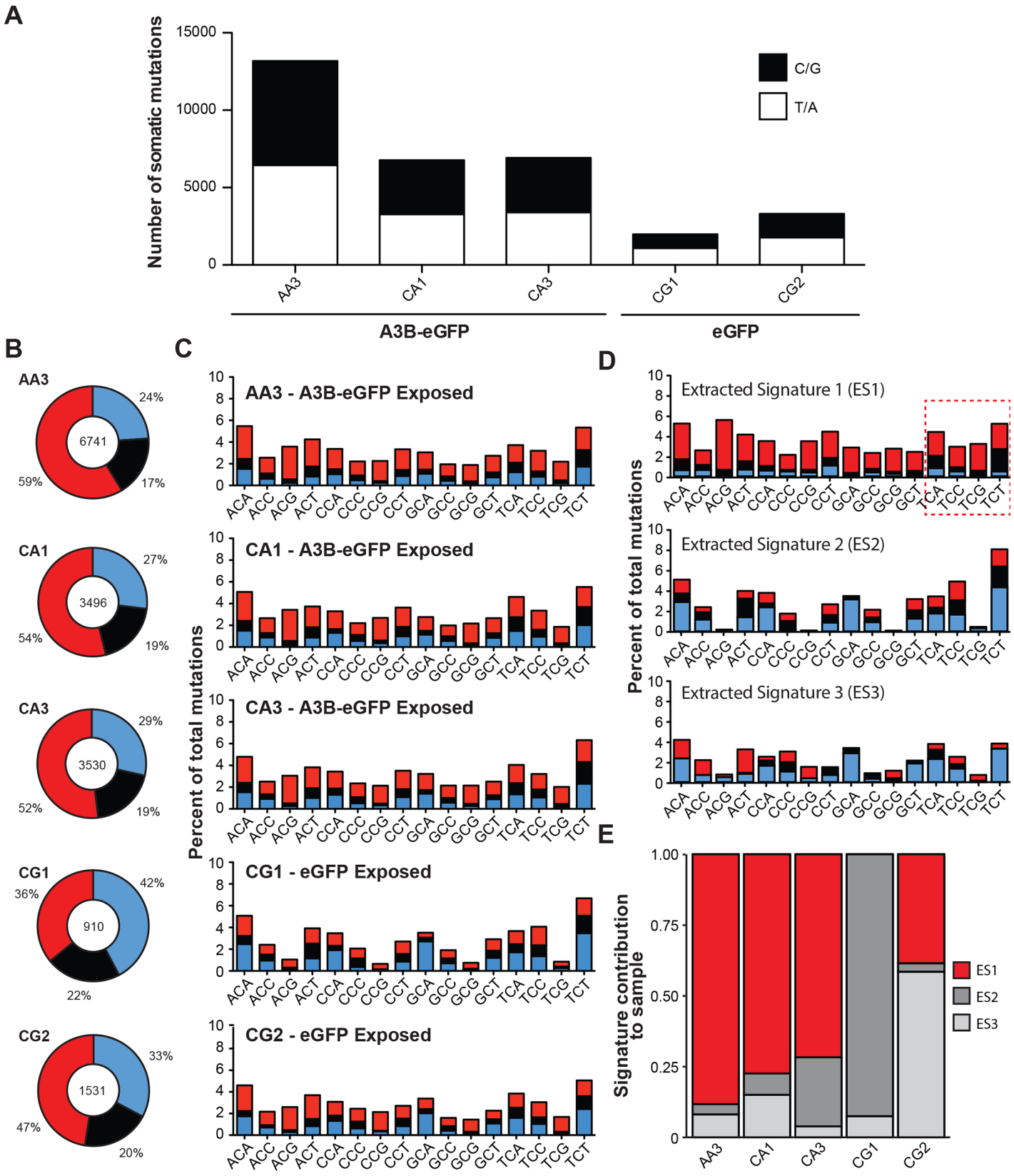
A
Number of somatic mutations
15000
10000
5000
0
C/G
T/A
AA3
CA1
CA3
CG1
CG2
A3B-eGFP
eGFP
B
AA3
24%
6741
59%
17%
CA1
27%
3496
54%
19%
CA3
29%
3530
52%
19%
CG1
42%
36%
910
22%
CG2
33%
1531
47%
20%
C
AA3 - A3B-eGFP Exposed
CA1 - A3B-eGFP Exposed
CA3 - A3B-eGFP Exposed
CG1 - eGFP Exposed
CG2 - eGFP Exposed
Percent of total mutations
ACA ACC ACG ACT CCA CCC CCG CCT GCA GCC GCG GCT TCA TCC TCG TCT
D
Extracted Signature 1 (ES1)
Extracted Signature 2 (ES2)
Extracted Signature 3 (ES3)
Percent of total mutations
E
Signature contribution to sample
1.00
0.75
0.50
0.25
0
ES1
ES2
ES3
AA3
CA1
CA3
CG1
CG2

**Fig 4. Summary of somatic mutations detected by WGS.** (A) Stacked bar graphs representing total number of C/G and T/A context somatic mutations in the indicated granddaughter subclones (black and white bars, respectively). Sequences from granddaughter clone AG3 were used as a baseline to call mutations in AA3 (i.e., mutations for AG3 are not shown in bar format because WGS data from another control granddaughter clone were not available for comparison). (B) Pie charts representing the proportion of each type of cytosine mutation across the genome in the indicated granddaughter clones. Red, blue, and black wedges represent C-to-T, C-to-A, and C-to-G mutations, respectively. (C) Stacked bar graphs representing the observed percentage of C-context somatic trinucleotide mutations detected in each granddaughter clone from the B panel. (D) Stacked bar graphs representing the extracted mutation signatures from WGS data. (E) The relative proportion that each extracted mutation signature contributes to the overall base substitution spectrum in the indicated granddaughter clones.

doi:10.1371/journal.pone.0155391.g004

## Discussion

A3B is emerging as a significant source of somatic mutation in many different cancer types (reviewed by [1–4] and see Introduction for references to primary literature). Here, we further develop a 293-based cellular system for conditional, Dox-mediated expression of A3B. The system was validated using flow cytometry, immunoblotting, enzyme activity assays, and, most importantly, three complementary mutation detection methods (3D-PCR, SNP array, and WGS). Our results demonstrated higher levels of cytosine-focused mutations in A3B-eGFP expressing cells, in comparison to eGFP controls. In particular, C-to-T transition mutations and C-to-G transversion mutations in A3B preferred trinucleotide motifs predominated after the composite mutation spectra were extracted into 3 separate signatures. These studies fortify the conclusion that A3B is a potent human genomic DNA mutagen.

An even more complex picture emerged by comparing the A3B-induced mutation signature with previously defined signatures [5]. ES1, which is attributable to A3B induction in this 293-based experimental system, clustered most closely to signature 1B, which is characterized by a dominant proportion of C-to-T transitions at NCG motifs attributed to spontaneous deamination of methyl-cytosine bases, rather than signatures 2 or 13, which are normally attributed to APOBEC. A previous study overexpressed A3B in a different 293-based system, and observed a similarly complex cytosine mutation distribution [22]. It is therefore possible that the intrinsic preference of A3B for deaminating TCA and TCG motifs may be skewed in living cells by downstream repair pathways or other mutation generating processes. In addition, although the 293-based system used here showed evidence for some sort of repair deficiency (below), ES2 and ES3 appeared most similar to signatures 5 and 16, which currently have no known etiology. Thus, the WGS data from this 293-based system indicated that the overall "APOBEC" signature is likely to be more complex than inferred by prior studies.

An unexpected outcome of our studies was the discovery of a significant preexisting mutation process operating in this 293-based system. It is likely attributable to a defect in replicative DNA polymerase proofreading function and/or in mismatch repair evident by microsatellite instability and pronounced base substitution mutation biases. However, the molecular nature of this defect is not obvious and may be genetic and/or epigenetic. For instance, the WGS data show 6 exonic and over 100 intronic alterations to mismatch repair and related genes that could induce such a mutator phenotype. These results are consistent with a prior WGS study that found 1000's of mutation differences between 6 different 293-derived cell lines, as well as significant down-regulation of MLH1 and MLH3 in a subset of lines [53]. Our studies are also consistent with at least two additional prior reports characterizing the related 293T cell line as mismatch repair defective [54, 55]. Regardless of the precise molecular explanation, given the large number of labs worldwide that rely upon 293 or 293-derived cell lines, knowledge of this mutator phenotype is likely to be helpful for informing future experimental designs using this system.

Despite a compelling case for A3B in cancer mutagenesis (key results cited in **Introduction**), the overall APOBEC mutation signature in cancer cannot be explained by A3B alone, because it is still evident in breast cancers lacking the entirety of the *A3B* gene due to a common

deletion polymorphism [56]. One or more of the other APOBEC family members with an intrinsic preference for 5'TC dinucleotide substrates may be responsible. A leading candidate is A3A due to high catalytic activity in biochemical assays, nuclear/cell-wide localization in some cell types, propensity to induce a DNA damage response and cell death upon overexpression, and the resemblance of its mutation signature in model systems to the observed APOBEC signature in many cancers [13, 19, 21, 33, 39, 42, 57–63]. *A3A* gene expression may also be derepressed as a side-affect of the *A3B* gene deletion [64]. Additional studies will be needed to unambiguously delineate the identities of the full repertoire of cancer-relevant APOBEC3 enzymes, quantify their relative contributions to mutation in each cancer type, and build upon this fundamental knowledge to improve cancer diagnostics and therapeutics.

## Supporting Information

**S1 Fig. T-to-C mutations in all samples exhibit a DNA replication strand bias similar to that observed in MSI cancers.**
(PDF)

**S1 Table. Somatic mutations from WGS of 293-based clones.**
(XLSX)

## Acknowledgments

We thank Emily Law for providing A3B-eGFP and eGFP constructs and several Harris and Grigoriadis lab members for helpful comments.

## Author Contributions

Conceived and designed the experiments: RSH AG MKA GJS. Performed the experiments: MKA GJS JSQ. Analyzed the data: MKA GJS JSQ NAT MAC ANJT AG RSH. Contributed reagents/materials/analysis tools: MAC. Wrote the paper: MKA GJS JSQ AG RSH.

## References

1. Roberts SA, Gordenin DA. Hypermutation in human cancer genomes: footprints and mechanisms. Nature reviews. 2014; 14(12):786–800. doi: 10.1038/nrc3816 PMID: 25417590.
2. Swanton C, McGranahan N, Starrett GJ, Harris RS. APOBEC enzymes: mutagenic fuel for cancer evolution and heterogeneity. Cancer Discov. 2015; 5(7):704–12. doi: 10.1158/2159-8290.CD-15-0344 PMID: 26091828; PubMed Central PMCID: PMC4497973.
3. Henderson S, Fenton T. APOBEC3 genes: retroviral restriction factors to cancer drivers. Trends Mol Med. 2015; 21(5):274–84. doi: 10.1016/j.molmed.2015.02.007 PMID: 25820175.
4. Helleday T, Eshtad S, Nik-Zainal S. Mechanisms underlying mutational signatures in human cancers. Nat Rev Genet. 2014; 15(9):585–98. doi: 10.1038/nrg3729 PMID: 24981601.
5. Alexandrov LB, Nik-Zainal S, Wedge DC, Aparicio SA, Behjati S, Biankin AV, et al. Signatures of mutational processes in human cancer. Nature. 2013; 500(7463):415–21. Epub 2013/08/16. doi: 10.1038/nature12477 nature12477 [pii]. PMID: 23945592.
6. Cleaver JE, Crowley E. UV damage, DNA repair and skin carcinogenesis. Front Biosci. 2002; 7:d1024–43. Epub 2002/03/19. PMID: 11897551.
7. Hecht SS. Lung carcinogenesis by tobacco smoke. Int J Cancer. 2012; 131(12):2724–32. Epub 2012/09/05. doi: 10.1002/ijc.27816 PMID: 22945513; PubMed Central PMCID: PMC3479369.
8. Poon SL, Pang ST, McPherson JR, Yu W, Huang KK, Guan P, et al. Genome-wide mutational signatures of aristolochic acid and its application as a screening tool. Sci Transl Med. 2013; 5(197):197ra01. doi: 10.1126/scitranslmed.3006086 PMID: 23926199.
9. Poon SL, Huang MN, Choo Y, McPherson JR, Yu W, Heng HL, et al. Mutation signatures implicate aristolochic acid in bladder cancer development. Genome medicine. 2015; 7(1):38. doi: 10.1186/s13073-015-0161-3 PMID: 26015808; PubMed Central PMCID: PMC4443665.

10. Lord CJ, Tutt AN, Ashworth A. Synthetic lethality and cancer therapy: lessons learned from the development of PARP inhibitors. Annu Rev Med. 2015; 66:455–70. doi: 10.1146/annurev-med-050913-022545 PMID: 25341009.

11. Nik-Zainal S, Alexandrov LB, Wedge DC, Van Loo P, Greenman CD, Raine K, et al. Mutational processes molding the genomes of 21 breast cancers. Cell. 2012; 149(5):979–93. Epub 2012/05/23. S0092-8674(12)00528-4 [pii] doi: 10.1016/j.cell.2012.04.024 PMID: 22608084.

12. Roberts SA, Sterling J, Thompson C, Harris S, Mav D, Shah R, et al. Clustered mutations in yeast and in human cancers can arise from damaged long single-strand DNA regions. Mol Cell. 2012; 46(4):424–35. doi: 10.1016/j.molcel.2012.03.030 PMID: 22607975; PubMed Central PMCID: PMC3361558.

13. Burns MB, Lackey L, Carpenter MA, Rathore A, Land AM, Leonard B, et al. APOBEC3B is an enzymatic source of mutation in breast cancer. Nature. 2013; 494(7437):366–70. Epub 2013/02/08. doi: 10.1038/nature11881 nature11881 [pii]. PMID: 23389445.

14. Burns MB, Temiz NA, Harris RS. Evidence for APOBEC3B mutagenesis in multiple human cancers. Nat Genet. 2013; 45(9):977–83. Epub 2013/07/16. doi: 10.1038/ng.2701 ng.2701 [pii]. PMID: 23852168.

15. Roberts SA, Lawrence MS, Klimczak LJ, Grimm SA, Fargo D, Stojanov P, et al. An APOBEC cytidine deaminase mutagenesis pattern is widespread in human cancers. Nat Genet. 2013; 45(9):970–6. doi: 10.1038/ng.2702 PMID: 23852170; PubMed Central PMCID: PMC3789062.

16. Albin JS, Harris RS. Interactions of host APOBEC3 restriction factors with HIV-1 in vivo: implications for therapeutics. Expert Rev Mol Med. 2010; 12:e4. Epub 2010/01/26. S1462399409001343 [pii] doi: 10.1017/S1462399409001343 PMID: 20096141; PubMed Central PMCID: PMC2860793.

17. Harris RS, Dudley JP. APOBECs and virus restriction. Virology. 2015;479–480C:131–45. doi: 10.1016/j.virol.2015.03.012 PMID: 25818029; PubMed Central PMCID: PMC4424171.

18. Bacolla A, Cooper DN, Vasquez KM. Mechanisms of base substitution mutagenesis in cancer genomes. Genes. 2014; 5(1):108–46. doi: 10.3390/genes5010108 PMID: 24705290; PubMed Central PMCID: PMC3978516.

19. Lackey L, Law EK, Brown WL, Harris RS. Subcellular localization of the APOBEC3 proteins during mitosis and implications for genomic DNA deamination. Cell Cycle. 2013; 12(5):762–72. Epub 2013/02/08. doi: 10.4161/cc.23713 23713 [pii]. PMID: 23388464; PubMed Central PMCID: PMC3610724.

20. Leonard B, Hart SN, Burns MB, Carpenter MA, Temiz NA, Rathore A, et al. APOBEC3B upregulation and genomic mutation patterns in serous ovarian carcinoma. Cancer Res. 2013; 73(24):7222–31. Epub 2013/10/25. doi: 10.1158/0008-5472.CAN-13-1753 PMID: 24154874; PubMed Central PMCID: PMC3867573.

21. Taylor BJ, Nik-Zainal S, Wu YL, Stebbings LA, Raine K, Campbell PJ, et al. DNA deaminases induce break-associated mutation showers with implication of APOBEC3B and 3A in breast cancer kataegis. Elife. 2013; 2:e00534. Epub 2013/04/20. doi: 10.7554/eLife.00534 00534 [pii]. PMID: 23599896; PubMed Central PMCID: PMC3628087.

22. Shinohara M, Io K, Shindo K, Matsui M, Sakamoto T, Tada K, et al. APOBEC3B can impair genomic stability by inducing base substitutions in genomic DNA in human cells. Sci Rep. 2012; 2:806. Epub 2012/11/15. doi: 10.1038/srep00806 PMID: 23150777; PubMed Central PMCID: PMC3496164.

23. Henderson S, Chakravarthy A, Su X, Boshoff C, Fenton TR. APOBEC-mediated cytosine deamination links PIK3CA helical domain mutations to human papillomavirus-driven tumor development. Cell Rep. 2014; 7(6):1833–41. doi: 10.1016/j.celrep.2014.05.012 PMID: 24910434.

24. de Bruin EC, McGranahan N, Mitter R, Salm M, Wedge DC, Yates L, et al. Spatial and temporal diversity in genomic instability processes defines lung cancer evolution. Science. 2014; 346(6206):251–6. doi: 10.1126/science.1253462 PMID: 25301630.

25. Sieuwerts AM, Willis S, Burns MB, Look MP, Meijer-Van Gelder ME, Schlicker A, et al. Elevated APOBEC3B correlates with poor outcomes for estrogen-receptor-positive breast cancers. Hormones & cancer. 2014; 5(6):405–13. doi: 10.1007/s12672-014-0196-8 PMID: 25123150; PubMed Central PMCID: PMC4228172.

26. Cescon DW, Haibe-Kains B, Mak TW. APOBEC3B expression in breast cancer reflects cellular proliferation, while a deletion polymorphism is associated with immune activation. Proc Natl Acad Sci U S A. 2015; 112(9):2841–6. doi: 10.1073/pnas.1424869112 PMID: 25730878.

27. Leonard B, McCann JL, Starrett GJ, Kosyakovsky L, Luengas EM, Molan AM, et al. The PKC/NF-kappaB signaling pathway induces APOBEC3B expression in multiple human cancers. Cancer Res. 2015; 75(21):4538–47. doi: 10.1158/0008-5472.CAN-15-2171-T PMID: 26420215; PubMed Central PMCID: PMC4631676.

28. Vieira VC, Leonard B, White EA, Starrett GJ, Temiz NA, Lorenz LD, et al. Human papillomavirus E6 triggers upregulation of the antiviral and cancer genomic DNA deaminase APOBEC3B. MBio. 2014; 5(6). doi: 10.1128/mBio.02234-14 PMID: 25538195; PubMed Central PMCID: PMC4278539.

29. Warren CJ, Xu T, Guo K, Griffin LM, Westrich JA, Lee D, et al. APOBEC3A functions as a restriction factor of human papillomavirus. J Virol. 2015; 89(1):688–702. doi: 10.1128/JVI.02383-14 PMID: 25355878; PubMed Central PMCID: PMC4301161.

30. Mori S, Takeuchi T, Ishii Y, Kukimoto I. Identification of APOBEC3B promoter elements responsible for activation by human papillomavirus type 16 E6. Biochem Biophys Res Commun. 2015; 460(3):555–60. doi: 10.1016/j.bbrc.2015.03.068 PMID: 25800874.

31. Periyasamy M, Patel H, Lai CF, Nguyen VT, Nevedomskaya E, Harrod A, et al. APOBEC3B-mediated cytidine deamination is required for estrogen receptor action in breast cancer. Cell Rep. 2015; 13 (1):108–21. doi: 10.1016/j.celrep.2015.08.066 PMID: 26411678; PubMed Central PMCID: PMC4597099.

32. Land AM, Wang J, Law EK, Aberle R, Kirmaier A, Krupp A, et al. Degradation of the cancer genomic DNA deaminase APOBEC3B by SIV Vif. Oncotarget. 2015; 6(37):39969–79. doi: 10.18632/oncotarget.5483 PMID: 26544511.

33. Carpenter MA, Li M, Rathore A, Lackey L, Law EK, Land AM, et al. Methylcytosine and normal cytosine deamination by the foreign DNA restriction enzyme APOBEC3A. J Biol Chem. 2012; 287(41):34801–8. Epub 2012/08/17. doi: 10.1074/jbc.M112.385161 M112.385161 [pii]. PMID: 22896697; PubMed Central PMCID: PMC3464582.

34. Suspène R, Aynaud MM, Guetard D, Henry M, Eckhoff G, Marchio A, et al. Somatic hypermutation of human mitochondrial and nuclear DNA by APOBEC3 cytidine deaminases, a pathway for DNA catabolism. Proc Natl Acad Sci U S A. 2011; 108(12):4858–63. Epub 2011/03/04. 1009687108 [pii] doi: 10.1073/pnas.1009687108 PMID: 21368204; PubMed Central PMCID: PMC3064337.

35. Rasmussen M, Sundstrom M, Goransson Kultima H, Botling J, Micke P, Birgisson H, et al. Allele-specific copy number analysis of tumor samples with aneuploidy and tumor heterogeneity. Genome Biol. 2011; 12(10):R108. doi: 10.1186/gb-2011-12-10-r108 PMID: 22023820; PubMed Central PMCID: PMC3333778.

36. Gehring JS, Fischer B, Lawrence M, Huber W. SomaticSignatures: inferring mutational signatures from single-nucleotide variants. Bioinformatics. 2015; 31(22):3673–5. doi: 10.1093/bioinformatics/btv408 PMID: 26163694.

37. Haradhvala NJ, Polak P, Stojanov P, Covington KR, Shinbrot E, Hess JM, et al. Mutational strand asymmetries in cancer genomes reveal mechanisms of DNA damage and repair. Cell. 2016; 164 (3):538–49. doi: 10.1016/j.cell.2015.12.050 PMID: 26806129; PubMed Central PMCID: PMC4753048.

38. Suspène R, Henry M, Guillot S, Wain-Hobson S, Vartanian JP. Recovery of APOBEC3-edited human immunodeficiency virus G->A hypermutants by differential DNA denaturation PCR. J Gen Virol. 2005; 86(Pt 1):125–9. PMID: 15604439.

39. Stenglein MD, Burns MB, Li M, Lengyel J, Harris RS. APOBEC3 proteins mediate the clearance of foreign DNA from human cells. Nat Struct Mol Biol. 2010; 17(2):222–9. PMID: 20062055. doi: 10.1038/nsmb.1744

40. Liu M, Duke JL, Richter DJ, Vinuesa CG, Goodnow CC, Kleinstein SH, et al. Two levels of protection for the B cell genome during somatic hypermutation. Nature. 2008; 451(7180):841–5. PMID: 18273020. doi: 10.1038/nature06547

41. Nilsen H, An Q, Lindahl T. Mutation frequencies and AID activation state in B-cell lymphomas from Ung-deficient mice. Oncogene. 2005; 24(18):3063–6. doi: 10.1038/sj.onc.1208480 PMID: 15735713.

42. Mussil B, Suspene R, Aynaud MM, Gauvrit A, Vartanian JP, Wain-Hobson S. Human APOBEC3A isoforms translocate to the nucleus and induce DNA double strand breaks leading to cell stress and death. PloS one. 2013; 8(8):e73641. doi: 10.1371/journal.pone.0073641 PMID: 23977391; PubMed Central PMCID: PMC3748023.

43. Ramiro AR, Jankovic M, Eisenreich T, Difilippantonio S, Chen-Kiang S, Muramatsu M, et al. AID is required for c-myc/IgH chromosome translocations in vivo. Cell. 2004; 118(4):431–8. PMID: 15315756.

44. Rucci F, Cattaneo L, Marrella V, Sacco MG, Sobacchi C, Lucchini F, et al. Tissue-specific sensitivity to AID expression in transgenic mouse models. Gene. 2006; 377:150–8. doi: 10.1016/j.gene.2006.03.024 PMID: 16787714.

45. Komori J, Marusawa H, Machimoto T, Endo Y, Kinoshita K, Kou T, et al. Activation-induced cytidine deaminase links bile duct inflammation to human cholangiocarcinoma. Hepatology. 2008; 47(3):888–96. doi: 10.1002/hep.22125 PMID: 18306229.

46. Matsumoto Y, Marusawa H, Kinoshita K, Endo Y, Kou T, Morisawa T, et al. Helicobacter pylori infection triggers aberrant expression of activation-induced cytidine deaminase in gastric epithelium. Nat Med. 2007; 13(4):470–6. doi: 10.1038/nm1566 PMID: 17401375.

47. Koboldt DC, Zhang Q, Larson DE, Shen D, McLellan MD, Lin L, et al. VarScan 2: somatic mutation and copy number alteration discovery in cancer by exome sequencing. Genome Res. 2012; 22(3):568–76. doi: 10.1101/gr.129684.111 PMID: 22300766; PubMed Central PMCID: PMC3290792.

48. Cibulskis K, Lawrence MS, Carter SL, Sivachenko A, Jaffe D, Sougnez C, et al. Sensitive detection of somatic point mutations in impure and heterogeneous cancer samples. Nat Biotechnol. 2013; 31 (3):213–9. doi: 10.1038/nbt.2514 PMID: 23396013; PubMed Central PMCID: PMC3833702.

49. Di Noia JM, Neuberger MS. Molecular mechanisms of antibody somatic hypermutation. Annu Rev Biochem. 2007; 76:1–22. PMID: 17328676.

50. Rayner E, van Gool IC, Palles C, Kearsey SE, Bosse T, Tomlinson I, et al. A panoply of errors: polymerase proofreading domain mutations in cancer. Nature reviews. 2016; 16(2):71–81. doi: 10.1038/nrc.2015.12 PMID: 26822575.

51. Boland CR, Goel A. Microsatellite instability in colorectal cancer. Gastroenterology. 2010; 138 (6):2073–87 e3. doi: 10.1053/j.gastro.2009.12.064 PMID: 20420947; PubMed Central PMCID: PMC3037515.

52. Harris RS. Molecular mechanism and clinical impact of APOBEC3B-catalyzed mutagenesis in breast cancer. Breast Cancer Res. 2015; 17:8. doi: 10.1186/s13058-014-0498-3 PMID: 25848704; PubMed Central PMCID: PMC4303225.

53. Lin YC, Boone M, Meuris L, Lemmens I, Van Roy N, Soete A, et al. Genome dynamics of the human embryonic kidney 293 lineage in response to cell biology manipulations. Nat Commun. 2014; 5:4767. doi: 10.1038/ncomms5767 PMID: 25182477; PubMed Central PMCID: PMC4166678.

54. Roesner LM, Mielke C, Fahnrich S, Merkhoffer Y, Dittmar KE, Drexler HG, et al. Stable expression of MutLgamma in human cells reveals no specific response to mismatched DNA, but distinct recruitment to damage sites. J Cell Biochem. 2013; 114(10):2405–14. doi: 10.1002/jcb.24591 PMID: 23696135.

55. Trojan J, Zeuzem S, Randolph A, Hemmerle C, Brieger A, Raedle J, et al. Functional analysis of hMLH1 variants and HNPCC-related mutations using a human expression system. Gastroenterology. 2002; 122(1):211–9. PMID: 11781295.

56. Nik-Zainal S, Wedge DC, Alexandrov LB, Petljak M, Butler AP, Bolli N, et al. Association of a germline copy number polymorphism of APOBEC3A and APOBEC3B with burden of putative APOBEC-dependent mutations in breast cancer. Nat Genet. 2014; 46(5):487–91. doi: 10.1038/ng.2955 PMID: 24728294; PubMed Central PMCID: PMC4137149.

57. Chen H, Lilley CE, Yu Q, Lee DV, Chou J, Narvaiza I, et al. APOBEC3A is a potent inhibitor of adeno-associated virus and retrotransposons. Curr Biol. 2006; 16(5):480–5. PMID: 16527742.

58. Thielen BK, McNevin JP, McElrath MJ, Hunt BV, Klein KC, Lingappa JR. Innate immune signaling induces high levels of TC-specific deaminase activity in primary monocyte-derived cells through expression of APOBEC3A isoforms. J Biol Chem. 2010; 285(36):27753–66. Epub 2010/07/10. M110.102822 [pii] doi: 10.1074/jbc.M110.102822 PMID: 20615867; PubMed Central PMCID: PMC2934643.

59. Hultquist JF, Lengyel JA, Refsland EW, LaRue RS, Lackey L, Brown WL, et al. Human and rhesus APOBEC3D, APOBEC3F, APOBEC3G, and APOBEC3H demonstrate a conserved capacity to restrict Vif-deficient HIV-1. J Virol. 2011; 85(21):11220–34. Epub 2011/08/13. JVI.05238-11 [pii] doi: 10.1128/JVI.05238-11 PMID: 21835787; PubMed Central PMCID: PMC3194973.

60. Aynaud MM, Suspene R, Vidalain PO, Mussil B, Guetard D, Tangy F, et al. Human Tribbles 3 protects nuclear DNA from cytidine deamination by APOBEC3A. J Biol Chem. 2012; 287(46):39182–92. Epub 2012/09/15. doi: 10.1074/jbc.M112.372722 M112.372722 [pii]. PMID: 22977230; PubMed Central PMCID: PMC3493958.

61. Land AM, Law EK, Carpenter MA, Lackey L, Brown WL, Harris RS. Endogenous APOBEC3A DNA cytosine deaminase is cytoplasmic and nongenotoxic. J Biol Chem. 2013; 288(24):17253–60. Epub 2013/05/04. doi: 10.1074/jbc.M113.458661 M113.458661 [pii]. PMID: 23640892; PubMed Central PMCID: PMC3682529.

62. Shee C, Cox BD, Gu F, Luengas EM, Joshi MC, Chiu LY, et al. Engineered proteins detect spontaneous DNA breakage in human and bacterial cells. Elife. 2013; 2:e01222. doi: 10.7554/eLife.01222 PMID: 24171103; PubMed Central PMCID: PMC3809393.

63. Chan K, Roberts SA, Klimczak LJ, Sterling JF, Saini N, Malc EP, et al. An APOBEC3A hypermutation signature is distinguishable from the signature of background mutagenesis by APOBEC3B in human cancers. Nat Genet. 2015; 47(9):1067–72. doi: 10.1038/ng.3378 PMID: 26258849.

64. Caval V, Suspene R, Shapira M, Vartanian JP, Wain-Hobson S. A prevalent cancer susceptibility APOBEC3A hybrid allele bearing APOBEC3B 3'UTR enhances chromosomal DNA damage. Nat Commun. 2014; 5:5129. doi: 10.1038/ncomms6129 PMID: 25298230.

HEALTH AND MEDICINE



# The DNA cytosine deaminase APOBEC3B promotes tamoxifen resistance in ER-positive breast cancer

Emily K. Law,[1,2,3,4]* Anieta M. Sieuwerts,[5]* Kelly LaPara,[2] Brandon Leonard,[2,3,4] Gabriel J. Starrett,[2,3,4] Amy M. Molan,[2,3,4] Nuri A. Temiz,[2,3,4] Rachel Isaksson Vogel,[2,6] Marion E. Meijer-van Gelder,[5] Fred C. G. J. Sweep,[7] Paul N. Span,[8] John A. Foekens,[5] John W. M. Martens,[5] Douglas Yee,[2] Reuben S. Harris[1,2,3,4†]

**Breast tumors often display extreme genetic heterogeneity characterized by hundreds of gross chromosomal aberrations and tens of thousands of somatic mutations. Tumor evolution is thought to be ongoing and driven by multiple mutagenic processes. A major outstanding question is whether primary tumors have preexisting mutations for therapy resistance or whether additional DNA damage and mutagenesis are necessary. Drug resistance is a key measure of tumor evolvability. If a resistance mutation preexists at the time of primary tumor presentation, then the intended therapy is likely to fail. However, if resistance does not preexist, then ongoing mutational processes still have the potential to undermine therapeutic efficacy. The antiviral enzyme APOBEC3B (apolipoprotein B mRNA-editing enzyme, catalytic polypeptide-like 3B) preferentially deaminates DNA C-to-U, which results in signature C-to-T and C-to-G mutations commonly observed in breast tumors. We use clinical data and xenograft experiments to ask whether APOBEC3B contributes to ongoing breast tumor evolution and resistance to the selective estrogen receptor modulator, tamoxifen. First, APOBEC3B levels in primary estrogen receptor–positive ($ER^+$) breast tumors inversely correlate with the clinical benefit of tamoxifen in the treatment of metastatic $ER^+$ disease. Second, APOBEC3B depletion in an $ER^+$ breast cancer cell line results in prolonged tamoxifen responses in murine xenograft experiments. Third, APOBEC3B overexpression accelerates the development of tamoxifen resistance in murine xenograft experiments by a mechanism that requires the enzyme's catalytic activity. These studies combine to indicate that APOBEC3B promotes drug resistance in breast cancer and that inhibiting APOBEC3B-dependent tumor evolvability may be an effective strategy to improve efficacies of targeted cancer therapies.**

## INTRODUCTION

Improvements in the detection and therapy of operable breast tumors have contributed to a steady decline in mortality (*1*, *2*). Essentially all breast cancer deaths are caused by metastatic outgrowths that compromise vital organs, such as the brain, liver, or lungs. Adjuvant systemic therapies effectively reduce the risk of recurrence at these distant metastatic sites by treating preexisting, clinically undetectable, micrometastatic deposits. In estrogen receptor–positive ($ER^+$) breast cancer, a propensity for late recurrence more than 5 years after surgery is well documented and has resulted in recommendations to extend adjuvant endocrine therapy for a total of 10 years (*3*, *4*). Although endocrine therapy may be extended, it is evident that late recurrences occur even while the patient is taking appropriate therapy (*5*). The late recurrence of these apparently dormant metastatic breast cancer cells may be due to ongoing tumor evolution and acquisition of additional genetic aberrations.

Mutations are thought to be the major drivers of recurrence, metastasis, and therapeutic resistance. Recent studies on the molecular origins of mutations in breast cancer have implicated several molecular mechanisms, including both spontaneous and enzyme-catalyzed deamination of DNA cytosine bases (*6*–*10*) [reviewed by Swanton *et al.* (*11*), Roberts and Gordenin (*12*), and Helleday *et al.* (*13*)]. The former process correlates with aging and is mostly due to hydrolytic conversion of 5-methyl cytosine (mC) bases within 5′ NmCG motifs into thymines, which escape base excision repair and are converted into C-to-T transition mutations by DNA replication (N = A, C, G, or T). The latter process is attributable to single-stranded DNA cytosine-to-uracil (C-to-U) deamination catalyzed by one or more members of the APOBEC3 (apolipoprotein B mRNA-editing enzyme, catalytic polypeptide-like 3) family of enzymes, characterized by C-to-T transitions and C-to-G transversions in 5′TCW motifs (W = A or T).

Human cells have the capacity to express up to seven distinct APOBEC3 enzymes, which function normally as overlapping innate immune defenses against a wide variety of DNA-based viruses and transposons [reviewed by Malim and Bieniasz (*14*), Stavrou and Ross (*15*), and Simon *et al.* (*16*)]. APOBEC3A (A3A) and APOBEC3B (A3B) are leading candidates for explaining APOBEC signature mutations in breast tumors because overexpression of these enzymes triggers DNA damage responses and inflicts chromosomal mutations in hallmark trinucleotide contexts (*7*, *17*–*21*). However, endogenous *A3A* is not expressed significantly, nor is its activity detectable in breast cancer cell lines (*7*, *22*) (see Results). The molecular relevance of A3A is therefore difficult to assess because the impact of the endogenous protein cannot be quantified. In comparison, endogenous A3B is predominantly nuclear and has been shown to be responsible for elevated levels of genomic uracil and mutation in multiple breast cancer cell lines (*7*, *22*). A3B is overexpressed in approximately 50%

[1]Howard Hughes Medical Institute, University of Minnesota, Minneapolis, MN 55455, USA. [2]Masonic Cancer Center, University of Minnesota, Minneapolis, MN 55455, USA. [3]Institute for Molecular Virology, University of Minnesota, Minneapolis, MN 55455, USA. [4]Department of Biochemistry, Molecular Biology and Biophysics, University of Minnesota, Minneapolis, MN 55455, USA. [5]Department of Medical Oncology and Cancer Genomics Netherlands, Erasmus MC Cancer Institute, 3015 GE Rotterdam, Netherlands. [6]Division of Gynecologic Oncology, Department of Obstetrics, Gynecology and Women's Health, University of Minnesota, Minneapolis, MN 55455, USA. [7]Department of Laboratory Medicine, Radboud University Medical Center, Nijmegen, Netherlands. [8]Department of Radiation Oncology, Radboud University Medical Center, Nijmegen, Netherlands.
*These authors contributed equally to this work.
†Corresponding author. Email: rsh@umn.edu

of primary breast tumors (*7*, *8*), and retrospective studies have associated elevated *A3B* mRNA levels with poor outcomes for adjuvant treatment–naïve ER$^+$ breast cancer cohorts (*23*, *24*). Our original studies relied on a retrospective prognostic analysis of a treatment-naïve ER$^+$ breast cancer cohort (*23*); therefore, the observed correlation between elevated *A3B* mRNA levels and poor clinical outcomes is consistent with a variety of therapy-independent intrinsic molecular mechanisms ranging from indirect models (such as A3B promoting tumor cell growth) to direct models (such as A3B causing the genomic DNA damage that results in mutations that fuel ongoing tumor evolution).

A current debate in the cancer field is whether the mutations that cause therapy resistance preexist in primary tumors (that is, exist even before diagnosis) or continually accumulate (even after treatment initiation). In support of the former view, primary tumors are often composed of billions of cells that are highly heterogeneous, and deep-sequencing studies have found known drug resistance mutations before therapy initiation [for example, (*25*–*27*)]. However, many studies also support the latter view of ongoing tumor evolution. For instance, primary tumor deep-sequencing studies often fail to find evidence for preexisting resistance mutations [for example, (*26*, *28*)]. Recurrent breast tumors also often have many more somatic mutations compared to corresponding primary tumors, suggesting ongoing and cumulative mutational processes (*29*, *30*). In addition, the subclonal nature of most mutations in breast cancer, as well as many other cancer types, provides strong evidence for ongoing tumor evolution, including significant proportions of APOBEC signature mutations (*28*, *31*, *32*). Moreover, at the clinical level, the fact that remission periods in breast cancer can last for many years strongly suggests that additional genetic changes are required for at least one remaining tumor cell to manifest as recurrent disease (*3*, *4*). Here, we test the hypothesis that A3B contributes to ongoing tumor evolution and to the development of drug resistance mutations in ER$^+$ breast cancer.

## RESULTS

### Primary breast tumor *A3B* mRNA levels predict therapeutic failure upon tumor recurrence

To determine whether A3B contributes to endocrine therapy resistance, we evaluated the predictive potential of *A3B* expression in primary breast tumors from a total of 285 hormone therapy–naïve breast cancer patients who received tamoxifen as a first-line therapy for recurrent disease (*33*). A schematic of the study timeline is shown in Fig. 1A, and detailed patient characteristics are shown in table S1. Archived fresh-frozen primary tumor specimens were used to prepare total RNA, and reverse transcription quantitative polymerase chain reaction (RT-qPCR) was used to quantify *A3B* mRNA levels. These gene expression results were divided into four quartiles for subsequent clinical data analysis, with primary tumors of the upper quartile expressing an average of fourfold to sixfold more *A3B* mRNA than those in the lower quartile (dark blue versus red histogram bars, respectively, in Fig. 1B).

The progression-free survival (PFS) durations following recurrence and subsequent first-line tamoxifen therapy were compared for each of the four *A3B* expression groups. This analysis revealed a dose-response relationship, with the highest *A3B*-expressing group associating with the shortest PFS and with the lowest *A3B*-expressing group associating with the longest PFS (Fig. 1C; log-rank, $P < 0.0001$). The median PFS was 6.2 months for the highest *A3B*-expressing group and 14.5 months for the lowest *A3B*-expressing group [hazard ratio (HR) 2.40 (1.69 to 3.41); log-rank, $P < 0.0001$]. This result remained significant for high versus low A3B levels in

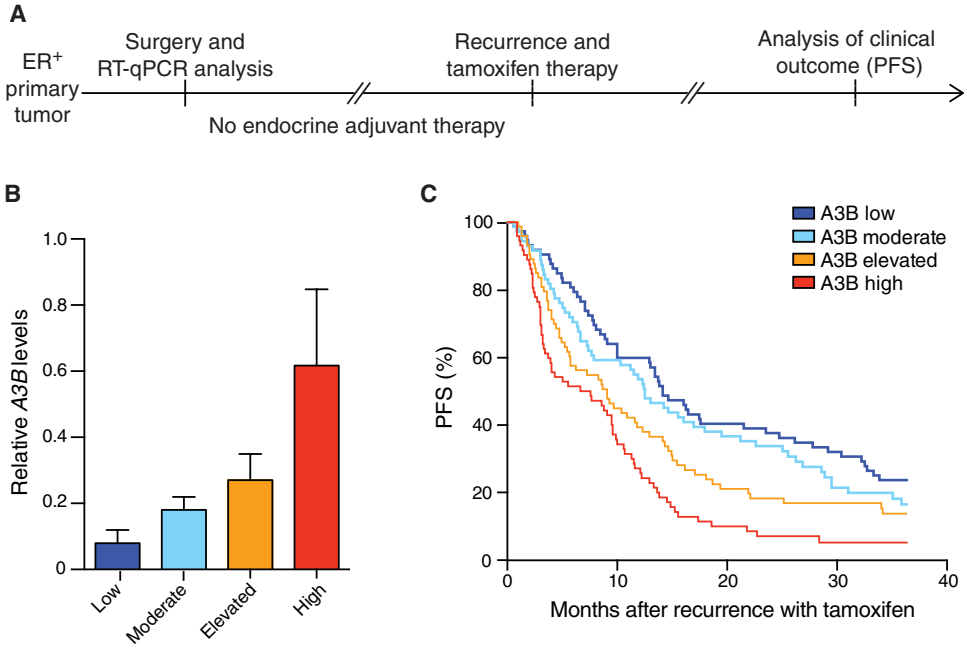


**Fig. 1. High *A3B* levels in primary ER$^+$ breast tumors predict poor response to tamoxifen therapy after tumor recurrence.** (**A**) Schematic of the clinical time course. Timeline breaks depict variable intervals between clinical milestones. (**B**) Relative *A3B* expression levels in each observation group [mean ± SD of $n = 72$ (quartiles 1 and 3), $n = 70$ (quartile 2), and $n = 71$ (quartile 4)]. (**C**) Kaplan-Meier curves showing the periods of PFS after initiating tamoxifen therapy for patients whose primary tumors expressed *A3B* at low (dark blue line), intermediate (light blue and orange lines), or high levels [red line; patient groups and color scheme match those in (B)].

a multivariate analysis after including the known clinical pathological predictors of age, disease-free interval, dominant site of relapse, adjuvant chemotherapy, and ER and progesterone receptor mRNA levels measured in the primary tumor [HR 2.19 (1.51 to 3.20); log-rank, $P < 0.0001$; table S2]. These data indicate that primary tumor *A3B* mRNA levels are strong and independent predictors of PFS for recurrent ER$^+$ breast cancer treated with tamoxifen. These observations do not support models in which resistance-conferring mutations preexist in primary tumors—or disease outcomes would have had no correlation with *A3B* expression levels and the data for each quartile group would have superimposed. Rather, the data support a model in which A3B promotes the ongoing diversification of residual primary tumor cells (micrometastatic deposits) that ultimately manifest in the recurrent setting as acquired resistance, failed tamoxifen therapy, and disease progression.

### Endogenous *A3B* depletion does not alter the phenotype of MCF-7L ER$^+$ breast cancer cells in culture

MCF-7 has been used for decades as a unique cell-based model for ER$^+$ breast cancer research [reviewed by Lee *et al.* (*34*)]. Engrafted MCF-7 tumors are dependent on ER function and therefore are sensitive to selective ER modulators, including tamoxifen. Furthermore, tamoxifen-induced tumor dormancy (indolence) in this model system, which can last for several months, frequently leads to drug-resistant and highly proliferative cell masses. For further studies, including animal experiments below, we elected to use the derivative line MCF-7L because it is tumorigenic in immunodeficient mice [Ibrahim *et al.* (*35*), Sachdev *et al.* (*36*), and references therein] and expresses endogenous *A3B* mRNA at levels approximating those found in many primary breast tumors (*7*). Like most other breast cancer cell lines, MCF-7L cells have very low levels of *A3A* and variable levels of other *APOBEC3* mRNAs, which have not been implicated in breast cancer mutagenesis (fig. S1).

We initially asked whether endogenous *A3B* depletion alters molecular or cellular characteristics of MCF-7L. Cells were transduced with an *A3B*-specific short hairpin RNA (shRNA) construct (shA3B) or a nonspecific shRNA construct as a control (shCON) (*7*), and uniform shRNA-expressing pools were selected using the linked puromycin resistance gene. In all shA3B-transduced pools, a robust >25-fold depletion of endogenous *A3B* mRNA was achieved (Fig. 2A). Moreover, the depletion of *A3B* mRNA was mirrored by a corresponding ablation of all measurable DNA cytosine deaminase activities from whole-cell and nuclear extracts (Fig. 2B). Although several other *APOBEC* family member genes are expressed in MCF-7L, their protein levels are likely too low to detect using this assay (A3A, A3D, A3G, and A1), the enzyme is not active on DNA (A2), and/or their single-stranded DNA cytosine deaminase activity is not evident in cellular extracts (A3C and A3F) (*7*, *22*). At the microscopic level, shA3B- and shCON-expressing cells were visibly indistinguishable (Fig. 2C). The two cell populations showed nearly identical growth rates and doubling times in cell culture (Fig. 2, D and E). These results are consistent with *A3B* knockdown data using the same shRNA construct in other breast cancer cell lines (*7*, *22*) and with the observation that *A3B* is a nonessential human gene (*37*).

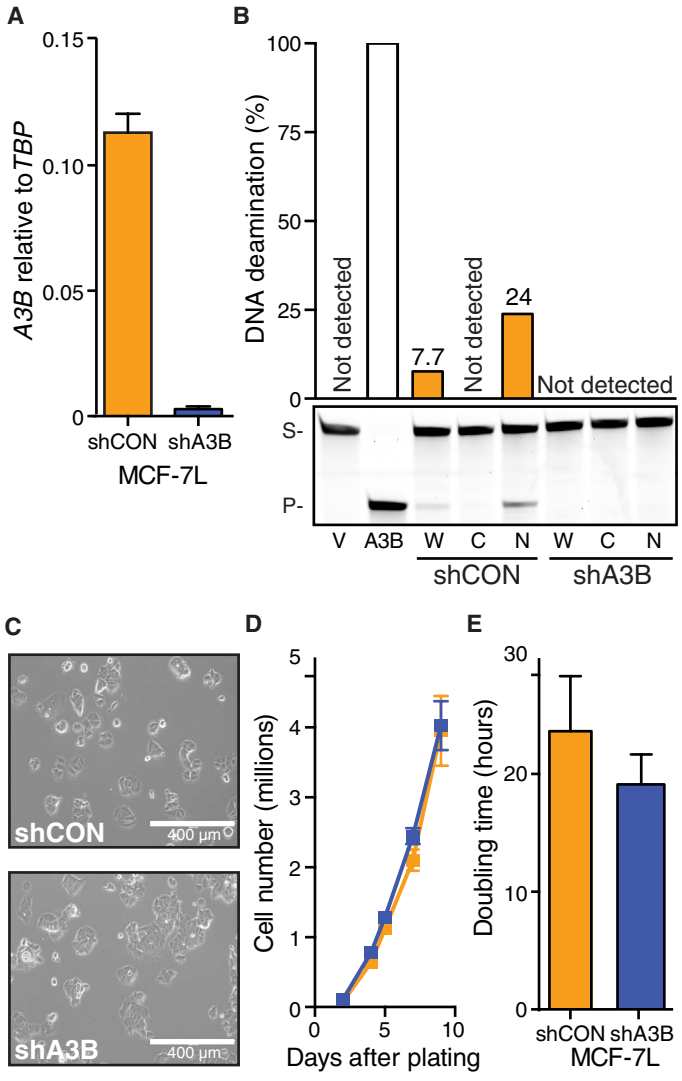


**Fig. 2. Endogenous *A3B* depletion does not alter MCF-7L ER$^+$ breast cancer cells in culture.** (**A**) *A3B* mRNA levels in MCF-7L cells expressing shA3B or shCON constructs (*TBP*, TATA-binding protein mRNA; each bar represents the mean ± SD of three RT-qPCR assays). (**B**) A3B DNA cytosine deaminase activity in soluble whole-cell (W), cytoplasmic (C), and nuclear (N) extracts of MCF-7L cells expressing shA3B or shCON constructs. Vector (V) and A3B-transfected 293T cell lysates were used as controls (S, substrate; P, product). (**C**) Light microscopy images of shA3B and shCON expressing MCF-7L pools. (**D** and **E**) Growth kinetics and doubling times of cultured MCF-7L cells expressing shA3B versus shCON constructs (mean ± SD of $n = 6$ cultures per condition).

### A3B is required for the development of tamoxifen-resistant tumors in mice

The clinical data reported in Fig. 1 support a model in which A3B is responsible for precipitating the mutations that promote tamoxifen resistance. To directly test this model, we performed a series of xenograft experiments using MCF-7L pools in which endogenous *A3B* was left intact (shCON) or was depleted with the specific shRNA described above (shA3B). For each condition, 5 million cells were injected subcutaneously into the flank regions of a cohort of 5-week-old immunodeficient mice, and tumors were allowed to reach a volume of approximately 150 mm$^3$. At this point, typically 40 to 50 days after engraftment, the mice in each experimental group were randomly assigned into two subcohorts, one to receive daily tamoxifen injections and the other to be observed in parallel as a control (schematic of experimental design in Fig. 3A).

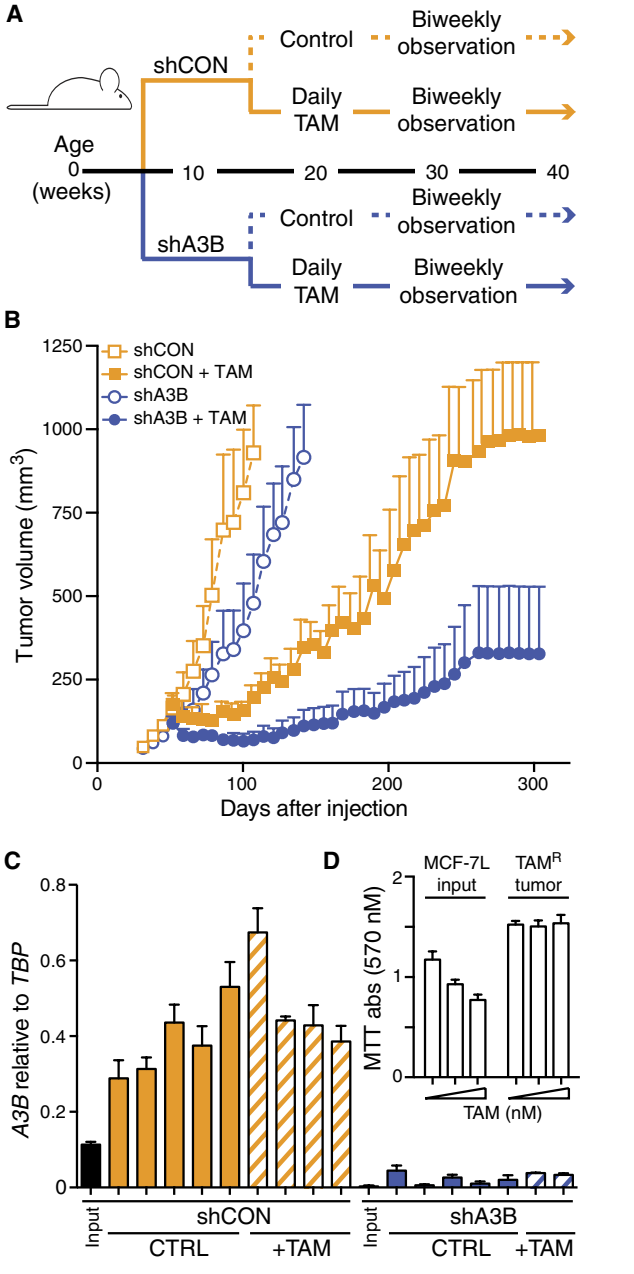


**Fig. 3. A3B is required for the development of tamoxifen-resistant tumors in mice.** (**A**) Schematic of the *A3B* knockdown xenograft study design and time course (see text for details). (**B**) Growth kinetics of engrafted MCF-7L cells expressing shA3B or shCON in the absence or presence of tamoxifen (TAM) treatment. Tumor volumes were measured weekly (mean + SEM shown for clarity of data presentation). (**C**) *A3B* mRNA levels in xenografted tumors recovered from the experiment shown in (B) (*TBP* mRNA; each bar represents the mean ± SD of three RT-qPCR assays). (**D**) MTT [3-(4,5-dimethylthiazol-2-yl)-2,5-diphenyltetrazolium bromide] data comparing tamoxifen susceptibility of input MCF-7L cells versus tamoxifen resistance of a representative MCF-7L shCON tumor [tamoxifen (10, 100, and 1000 ng/ml)].

Control-transduced MCF-7L cells formed large 1000-mm$^3$ tumors within 100 days after engraftment and, interestingly, *A3B* knockdown caused a modest delay in tumor growth (open blue versus open orange symbols in Fig. 3B; linear mixed model, *F* test, $P = 0.002$). This result differed from the near-identical growth rates in cell culture (Fig. 2, D and E) and may be due to the likelihood that additional adaptations/mutations are required for monolayer/plastic-conditioned cells to be able to grow optimally as tumors in mice. As expected, tamoxifen treatment attenuated the growth of both engineered pools (filled orange and blue symbols in Fig. 3B). However, control-transduced cells rapidly developed resistance to tamoxifen and grew into large tumors, whereas the growth of the *A3B*-depleted cell masses was mostly suppressed by tamoxifen over the year-long duration of this representative experiment (filled orange versus blue symbols in Fig. 3B; linear mixed model, *F* test, $P < 0.0001$). Similar outcomes were observed in additional experiments (for example, fig. S2).

Xenograft tumor *A3B* mRNA levels were analyzed by RT-qPCR, and, in all instances, the intended knockdown or control mRNA level was found to be durable and maintained through the entire duration of the experiment (Fig. 3C). This series of control experiments also revealed that endogenous *A3B* mRNA levels increase in control shRNA–transduced tumor masses in comparison to the same cells before engraftment (Fig. 3C). The mechanism for *A3B* induction in immunodeficient mice is not known but is unlikely to be due to estrogen (figs. S3 and S4), as suggested by a recent report (*38*). Representative xenografts were recovered in culture, and the tamoxifen-resistant phenotype was reconfirmed (for example, Fig. 3D). These results are fully supportive of a mechanism in which endogenous A3B causes an inheritable drug resistance phenotype (addressed further below). It is notable that endogenous *A3B* mRNA levels in this system are comparable to those observed in a large proportion of primary tumors [approximately 0.1 to 0.2 relative to *TBP* mRNA levels in cultured MCF-7L cells (Fig. 2B), 0.4 relative to *TBP* in animal tumors described here (Fig. 3C and fig. S3), and a range of 0 to 1.25 and a median of 0.25 relative to *TBP* in primary breast tumors previously documented using the same RT-qPCR assay (*7*)].

## A novel lentivirus-based system enables A3B overexpression in any cell type

We next developed a conditional A3B overexpression system to further test the A3B mutagenesis model. A conditional approach is required because A3B expression in virus-producing cells causes lethal mutagenesis of retroviral complementary DNA intermediates during reverse transcription (*39*–*42*), and excessive levels of cellular A3B have the potential to inflict genomic DNA damage that ultimately leads to cytotoxicity (*7*, *18*, *19*). We therefore developed a novel lentiviral construct that will only express A3B upon transduction into susceptible target cells (Fig. 4A). This construct mitigates viral toxicity issues because it is inactive in virus-producing cells as a result of disruption of the antisense *A3B* open reading frame with a sense strand intron, and it is only expressed after intron removal by splicing in the virus-producing cells and reverse transcription and integration of the full proviral DNA in susceptible target cells. It also mitigates toxicity issues for target cell populations because expression levels are not excessive (see below). In parallel, an A3B catalytic mutant derivative (E255Q) was created by site-directed mutagenesis to serve as a negative control.

Transducing viruses were made by plasmid transfection into 293T cells with appropriate retroviral helper plasmids encoding Gag, Pol, and Env (vesicular stomatitis virus glycoprotein). As anticipated, no producer cell toxicity was observed, and A3B and A3B-E255Q viral titers were equivalent by RT-qPCR. MCF-7L cells were transduced

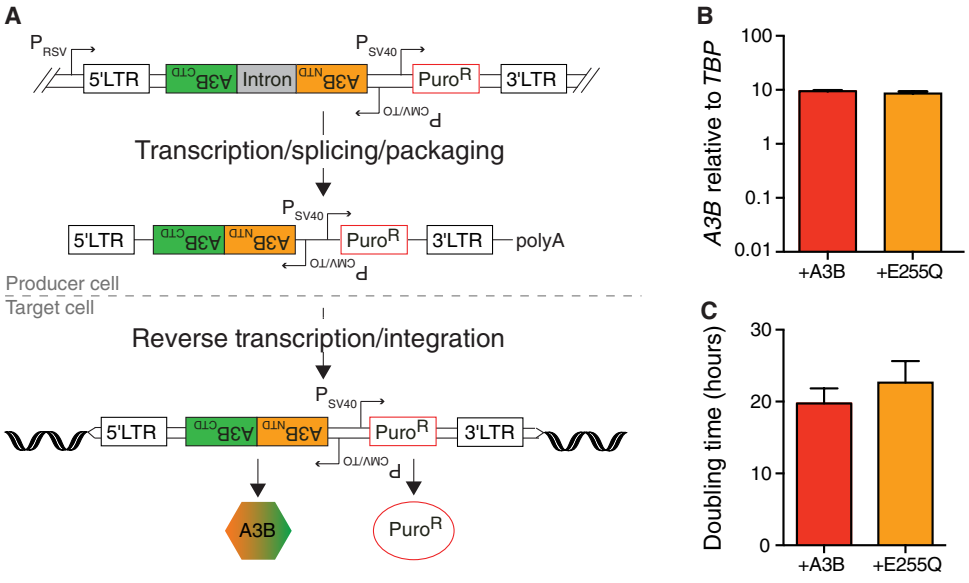


**Fig. 4. Novel lentivirus-based system for conditional A3B overexpression.** (**A**) Schematic of the lentiviral construct for conditional *A3B* overexpression (see text for details). LTR, long terminal repeat; RSV, Rous sarcoma virus; CTD, C-terminal domain; NTD, N-terminal domain; CMV, cytomegalovirus; SV40, simian virus 40. (**B**) *A3B* mRNA levels relative to *TBP* in MCF-7L cells expressing lentivirus-delivered *A3B* or a catalytic mutant derivative (E255Q) as well as endogenous *A3B* (mean ± SD of three RT-qPCR assays). (**C**) Doubling times of cultured MCF-7L cells overexpressing A3B or A3B-E255Q (mean ± SD of four replicates).

with each virus stock, and puromycin selection was used to eliminate nontransduced cells and to ensure 100% transduction efficiencies. *A3B* quantification by RT-qPCR showed that each construct elevates mRNA expression to levels approximately 10-fold higher than those of the reference gene *TBP* (Fig. 4B), which equate to levels approximately 50-fold higher than those of the endogenous *A3B* expressed in this system. These *A3B* mRNA levels are similar to those found in the top fraction of breast tumors and cancer cell lines [Burns *et al.* (*7*), Leonard *et al.* (*22*), Sieuwerts *et al.* (*23*), and this study]. As for the *A3B* knockdown experiments above, A3B- and A3B-E255Q–overexpressing MCF-7L populations showed no overt signs of toxicity and indistinguishable growth rates (Fig. 4C).

## Overexpression of catalytically active A3B accelerates the development of tamoxifen-resistant tumors

To further test the model in which A3B provides mutagenic fuel for tumor evolution and drug resistance, we performed a series of xenograft experiments using MCF-7L cells transduced with the aforementioned constructs and thereby overexpressing wild-type A3B or the catalytic mutant derivative A3B-E255Q (Fig. 5A). Immunodeficient animals were injected subcutaneously with 5 million cells and, upon palpable tumor growth (150 $mm^3$), randomly divided into groups for tamoxifen injections or control observation. Remarkably, most of the cell masses overexpressing *A3B* developed rapid resistance to tamoxifen (filled red symbols in Fig. 5B). In comparison, MCF-7L cells expressing equivalent levels of *A3B-E255Q* mutant mRNA showed resistance kinetics similar to those of the shCON engraftments described above (filled orange symbols in Fig. 5B; linear mixed model, $F$ test, $P = 0.015$). An independent experiment yielded similar results (fig. S5). These data demonstrate that A3B overexpression accelerates the kinetics of the development of tamoxifen resistance and, notably, that this phenotype requires catalytic activity.

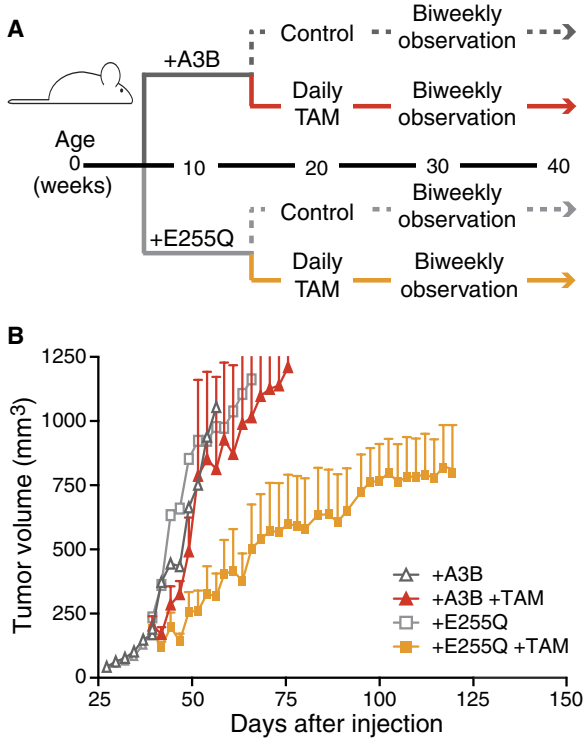


**Fig. 5. Overexpression of catalytically active A3B accelerates the development of tamoxifen-resistant tumors in mice.** (**A**) Schematic of the *A3B* overexpression xenograft study design and time course (see text for details). (**B**) Growth kinetics of engrafted MCF-7L cells overexpressing A3B or A3B-E255Q in the absence or presence of tamoxifen treatment. The graph reports tumor volumes measured weekly (mean + SEM shown for clarity of data presentation). Average tumor volumes from the untreated control arms are shown by gray symbols, and overlapping error bars are omitted for clarity of presentation.

### *ESR1* mutations are not responsible for tamoxifen resistance in the MCF-7L model for ER$^+$ breast cancer

Although the development of tamoxifen-resistant breast tumors is a major clinical problem, in most cases the molecular basis for resistance is unknown. A small fraction of treated patients develop tumors with *ESR1* exonic mutations that cause amino acid changes in the hormone-binding domain of the ER. These mutations have been seen mostly in tumors resistant to aromatase inhibitors and not as frequently in tumors resistant to tamoxifen [reviewed by Clarke *et al.* (*43*) and Jeselsohn *et al.* (*44*)]. To determine whether *ESR1* mutations are also part of the tamoxifen resistance mechanism in MCF-7L cells, we performed DNA exome sequencing on 9 independent tamoxifen-resistant xenografts and 10 independent control tumor masses. The *ESR1* gene contained no mutations under either condition (see table S3 for a full list of base substitution mutations). Resistant tumor *ESR1* mRNA levels were somewhat variable but still similar to those present in the original MCF-7L cell populations (fig. S6). Together with the data presented above indicating heritable resistance to tamoxifen (Fig. 3D), these results suggest that at least one other resistance mechanism occurs in the MCF-7 model system for ER$^+$ breast cancer.

## DISCUSSION

The clinical and xenograft results presented here strongly support a model in which A3B drives tamoxifen resistance in ER$^+$ breast cancer. Clinically, resistance to endocrine therapies has been defined as primary or secondary, depending on the length of time a patient benefits from ER-targeted therapy. Our data suggest that A3B may have a role in both kinds of resistance and particularly in the development of secondary, acquired resistance. Suppression of endogenous levels of A3B enhances tamoxifen benefit (Fig. 3), whereas overexpression of A3B eliminates almost all benefits from tamoxifen therapy (Fig. 5). Because the only known biochemical activity of A3B is single-stranded DNA cytosine deamination [for example, (*7*, *42*, *45*)] and the tamoxifen resistance phenotype is heritable (Fig. 3D), the most likely mechanism is A3B-catalyzed DNA C-to-U editing coupled to the processing of these uracil lesions into somatic mutations by normal DNA repair processes [reviewed by Swanton *et al.* (*11*), Roberts and Gordenin (*12*), and Helleday *et al.* (*13*)]. In further support of this mechanism, the catalytic glutamate of A3B (E255) is required for accelerated tamoxifen resistance kinetics upon enzyme overexpression.

Because *ESR1* mutations were not observed in MCF-7L tamoxifen-resistant tumors, the identity of the resistance-conferring mutations in this system will require significant future studies and possibly even whole-genome sequencing if the predominant causal lesions lie outside the exomic fraction of the genome. The intrinsic signature of A3B may help to identify candidate (frequently mutated) sites for mechanistic follow-up. Then, for instance, genetic knock-in experiments could be used to unambiguously establish a cause-effect relationship. However, the resistance-conferring mutations (such as gene translocations, amplifications, or deletions) could also be complex and difficult to recapitulate precisely because DNA repair enzymes can readily process genomic uracil lesions into single- and double-stranded breaks (*46*, *47*).

A3B has been implicated as a dominant source of mutation in breast, head/neck, lung, bladder, and cervical cancers and—to a lesser but still significant extent—in many other tumor types (*7*–*10*, *28*, *32*, *48*, *49*). The fundamental nature of the DNA deamination mechanism, together with the data presented here, strongly suggests that A3B may be a general mechanism of therapeutic resistance to cancer therapy. At this point, potential mutagenic contributions from other APOBEC3 family members, such as A3A, cannot be excluded fully, but they do not appear to manifest in the MCF-7L system, nor are these potential contributions large enough to prevent the significant association between *A3B* expression levels and clinical outcomes for ER$^+$ breast cancer patients [treatment-naïve data in the studies by Sieuwerts *et al.* (*23*) and Cescon *et al.* (*24*) and post-recurrence tamoxifen resistance data in Fig. 1]. Thus, strategies to down-regulate A3B activity or expression, as reported here using a specific shRNA knockdown construct in a model system for ER$^+$ breast cancer, may be beneficial as chemotherapeutic adjuvants to "turn down" the mutation rate, decrease the likelihood of evolving drug resistance, and prolong the clinical benefit of therapy for the many cancers that are likely to be driven by this ongoing mutational process.

## MATERIALS AND METHODS

### Clinical studies

The clinical characteristics of the 285 patients [225 from Rotterdam (Erasmus University Medical Center) and 60 from Nijmegen (Radboud University Medical Center)] whose primary tumor specimens and data were used here have been described previously by Sieuwerts *et al.* (*33*). The protocol to study biological markers associated with disease outcome was approved by the medical ethics committee of the Erasmus University Medical Center (Rotterdam, Netherlands) (MEC 02.953); for Nijmegen, coded primary tumor tissues were used in accordance with the Codes of Conduct of the Federation of Medical Scientific Societies in the Netherlands (www.federa.org/codes-conduct). Thirty-two patients presented with distant metastasis at diagnosis or developed distant metastasis (including supraclavicular lymph node metastasis) within 1 month following primary surgery (M1 patients). These 32 patients and the 253 patients who developed a first recurrence during follow-up (25 patients with local-regional relapse and 228 patients with distant metastasis) were treated with first-line tamoxifen. All patients were ER$^+$ and anti–hormonal therapy–naïve, but 38 patients received adjuvant chemotherapy. The median time between the primary surgery and the start of therapy was 24 months (range, 0 to 120 months). The median follow-up of patients alive at the end of follow-up was 98 months (range, 9 to 240 months) after the primary surgery and 45 months (range, 3 to 178 months) after the start of first-line tamoxifen therapy. For 182 patients (64%), disease progression occurred within 6 months of the start of the first-line therapy being controlled by tamoxifen. At the end of the follow-up period, 268 (94%) patients had developed tumor progression, and 222 (78%) patients had died.

Total RNA was extracted with RNA Bee (Tel Test, Thermo Fisher Scientific Inc.) from 30-μm fresh-frozen primary tumor tissue sections containing at least 30% invasive tumor cell nuclei, and mRNA transcripts were quantified by RT-qPCR as described previously by Sieuwerts *et al.* (*23*). The median *A3B* expression level in the group of 285 breast cancers was 0.22 relative to the normalized average of three reference genes [*HPRT1*, *HMBS*, and *TBP* (*23*)].

### DNA constructs

*A3B* knockdown and control shRNA constructs were described and validated previously by Burns *et al.* (*7*) and Leonard *et al.* (*50*). The A3B and A3B-E255Q lentiviral expression constructs were based

on the pLenti4TO backbone (Life Technologies). Overlapping PCR was used to place a sense-encoded intron between an antisense-encoded A3B open reading frame (primers available on request). A cytomegalovirus promoter drove A3B expression, and a simian virus 40 early promoter drove puromycin resistance. Constructs were verified by DNA sequencing.

### Cell culture studies

MCF-7L cells were cultured at 37°C under 5% $CO_2$ and maintained in improved minimum essential medium (Richter's modification medium) containing 5% fetal bovine serum, penicillin (100 U/ml), streptomycin (100 μg/ml), and 11.25 nM recombinant human insulin. These cells were originally obtained from C. Kent Osborne (Baylor College of Medicine, Houston, TX) and are subject to short tandem repeat analysis yearly to confirm their identity with the original MCF-7 cell line. Cells were transduced with the lentivirus-based shRNA or conditional expression constructs described above and selected with puromycin (1 μg/ml; United States Biological) for 72 hours to generate uniformly transduced pools. Cell growth experiments were performed by plating 100,000 cells per six-well plate and incubating them at 37°C for the indicated days. Cells were trypsinized, diluted 1:2 in trypan blue (Invitrogen), and counted via a hemocytometer (six biological replicates per day per condition). Cell proliferation rates were determined using the xCELLigence real-time cell analyzer dual-plate instrument according to the manufacturer's instructions (ACEA Biosciences).

The mRNA level of each *APOBEC* family member gene was quantified using previously described RT-qPCR protocols and primer/probe combinations and presented relative to the housekeeping gene *TBP* (*7*, *51*, *52*). *ESR1* and *C-MYC* RNA were quantified by RT-qPCR using intron-spanning primers 5′-ATGACCATGACCCTCCACACC and 5′-TCAGACCGTGGCAGGGAAACC (UPL24) and 5′-GCTGCTTAGACGCTGGATTT and 5′-TAACGTTGAGGGGCATCG (UPL66), respectively, and manufacturer-recommended protocols (LightCycler 480, Roche). *C-MYC* is an established estrogen-responsive gene (*53*).

DNA deaminase activity was measured in soluble whole-cell, nuclear, and cytoplasmic fractions of MCF-7L cultures using established protocols (*7*, *54*). The single-stranded DNA substrate contained a single target cytosine (5′-ATTATTATTATTCGAATGGATTTATTTATTTATTTATTTATTT-fluorescein); deamination, uracil excision, and backbone cleavage resulted in a single faster-migrating product on SDS–polyacrylamide gel electrophoresis and image analysis (Typhoon FLA 7000 and ImageQuant software, GE Healthcare Life Sciences).

### Xenograft studies

The University of Minnesota Institutional Animal Care and Use Committee approved the animal protocols used here (1305-30638A). MCF-7L cells were harvested at 70% confluence, counted, and resuspended in serum-free medium (without phenol red) at a concentration of 5 million cells per 50 μl of final volume. Ovariectomized, athymic mice (Harlan) were injected subcutaneously in the left flank with 50 μl of cell suspension at approximately 5 weeks of age. Each experiment was initiated with 5 or 10 mice per experimental condition. One week before injection and at all times following, the mice were provided with drinking water supplemented with 1 μM β-estradiol (Sigma-Aldrich) (except for the subset of mice used in the experiment shown in fig. S3). Tumors were measured bidirectionally twice weekly, and tamoxifen treatment began when the average tumor volume reached 150 $mm^3$. Tamoxifen citrate (500 μg; Sigma-Aldrich) emulsified in 50 μl of peanut oil was administered subcutaneously 5 of 7 days each week. Tumor volumes were calculated using the following formula: length × $breadth^2/2$.

### MCF-7L exome sequencing

Genomic DNA was prepared from tumor cell masses (~20 mg per sample) via the Gentra Puregene Tissue DNA isolation protocols (Qiagen). Samples were diluted to 100 ng/μl and assessed further for quality and purity by SYBR Green PCR on a 197-bp fragment of *A3H* using primers 5′-CATGGGACTGGACGAAGCGCA and 5′-TGGGATCCACACAGAAGCCGCA. Samples with no amplification were excluded from the analysis. One microgram of total genomic DNA per sample was subjected to whole-exome sequencing on the Complete Genomics platform to an average target depth of 100× (BGI). Reads were aligned by BGI using its in-house pipeline, and the alignments in bam format were used for variant calling. Somatic variants were called for each tumor alignment by VarScan 2 (*55*) using an estrogen-treated shA3B sample as the normal control. The variants were filtered with a minimum overall coverage depth of 20 reads and a minimum coverage depth of 4 reads for the alternate allele. Any variant occurring at any frequency above 0 at the same position in more than one sample was considered a common mutation in the input pool and was removed. A full list of base substitution mutations is provided in table S3.

### Statistics

Comparisons of the PFS of hormone-naïve breast cancer patients following treatment for first recurrence with tamoxifen, by *A3B* expression level (divided into quartiles), were conducted using log-rank tests; HRs and 95% confidence intervals are presented for pairwise comparisons. Clinical data were analyzed using SPSS Statistics version 23.0 (IBM). In the xenograft studies, repeated measures of tumor volume over time were compared by treatment group using linear mixed models with fixed effects for treatment, days, and interaction between treatment and days and with random intercept and slope effects for each mouse. $P$ values <0.05 were considered statistically significant. Xenograft data were analyzed using Prism 6 and SAS 9.3.

## SUPPLEMENTARY MATERIALS

Supplementary material for this article is available at http://advances.sciencemag.org/cgi/content/full/2/10/e1601737/DC1

fig. S1. APOBEC family member expression in MCF-7L cells.
fig. S2. Replica *A3B* knockdown xenograft experiment.
fig. S3. Estrogen does not affect *A3B* mRNA levels in engrafted MCF-7L cells.
fig. S4. *A3B* is not estrogen-inducible.
fig. S5. Replica *A3B* overexpression xenograft experiment.
fig. S6. *ESR1* mRNA levels in tamoxifen-resistant MCF-7L cells.
table S1. Patient characteristics and median and interquartile range of *APOBEC3B* mRNA levels.
table S2. Cox univariate and multivariate analyses for PFS after initiating first-line tamoxifen.
table S3. Single-base substitution mutations in tamoxifen-resistant tumors (separate Microsoft Excel file).

## REFERENCES AND NOTES

1. E. B. Elkin, C. A. Hudis, Parsing progress in breast cancer. *J. Clin. Oncol.* **33**, 2837–2838 (2015).
2. J. H. Park, W. F. Anderson, M. H. Gail, Improvements in US breast cancer survival and proportion explained by tumor size and estrogen-receptor status. *J. Clin. Oncol.* **33**, 2870–2876 (2015).

3. T. Saphner, D. C. Tormey, R. Gray, Annual hazard rates of recurrence for breast cancer after primary therapy. *J. Clin. Oncol.* **14**, 2738–2746 (1996).
4. H. J. Burstein, S. Temin, H. Anderson, T. A. Buchholz, N. E. Davidson, K. E. Gelmon, S. H. Giordano, C. A. Hudis, D. Rowden, A. J. Solky, V. Stearns, E. P. Winer, J. J. Griggs, Adjuvant endocrine therapy for women with hormone receptor–positive breast cancer: American Society of Clinical Oncology clinical practice guideline focused update. *J. Clin. Oncol.* **32**, 2255–2269 (2014).
5. C. Davies, H. Pan, J. Godwin, R. Gray, R. Arriagada, V. Raina, M. Abraham, V. H. Medeiros Alencar, A. Badran, X. Bonfill, J. Bradbury, M. Clarke, R. Collins, S. R. Davis, A. Delmestri, J. F. Forbes, P. Haddad, M.-F. Hou, M. Inbar, H. Khaled, J. Kielanowska, W. H. Kwan, B. S. Mathew, I. Mittra, B. Müller, A. Nicolucci, O. Peralta, F. Pernas, L. Petruzelka, T. Pienkowski, R. Radhika, B. Rajan, M. T. Rubach, S. Tort, G. Urrútia, M. Valentini, Y. Wang, R. Peto; Adjuvant Tamoxifen: Longer Against Shorter Collaborative, Long-term effects of continuing adjuvant tamoxifen to 10 years versus stopping at 5 years after diagnosis of oestrogen receptor-positive breast cancer: ATLAS, a randomised trial. *Lancet* **381**, 805–816 (2013).
6. S. Nik-Zainal, L. B. Alexandrov, D. C. Wedge, P. Van Loo, C. D. Greenman, K. Raine, D. Jones, J. Hinton, J. Marshall, L. A. Stebbings, A. Menzies, S. Martin, K. Leung, L. Chen, C. Leroy, M. Ramakrishna, R. Rance, K. W. Lau, L. J. Mudie, I. Varela, D. J. McBride, G. R. Bignell, S. L. Cooke, A. Shlien, J. Gamble, I. Whitmore, M. Maddison, P. S. Tarpey, H. R. Davies, E. Papaemmanuil, P. J. Stephens, S. McLaren, A. P. Butler, J. W. Teague, G. Jönsson, J. E. Garber, D. Silver, P. Miron, A. Fatima, S. Boyault, A. Langerød, A. Tutt, J. W. M. Martens, S. A. J. R. Aparicio, Å. Borg, A. V. Salomon, G. Thomas, A.-L. Børresen-Dale, A. L. Richardson, M. S. Neuberger, P. A. Futreal, P. J. Campbell, M. R. Stratton; Breast Cancer Working Group of the International Cancer Genome Consortium, Mutational processes molding the genomes of 21 breast cancers. *Cell* **149**, 979–993 (2012).
7. M. B. Burns, L. Lackey, M. A. Carpenter, A. Rathore, A. M. Land, B. Leonard, E. W. Refsland, D. Kotandeniya, N. Tretyakova, J. B. Nikas, D. Yee, N. A. Temiz, D. E. Donohue, R. M. McDougle, W. L. Brown, E. K. Law, R. S. Harris, APOBEC3B is an enzymatic source of mutation in breast cancer. *Nature* **494**, 366–370 (2013).
8. M. B. Burns, N. A. Temiz, R. S. Harris, Evidence for APOBEC3B mutagenesis in multiple human cancers. *Nat. Genet.* **45**, 977–983 (2013).
9. S. A. Roberts, M. S. Lawrence, L. J. Klimczak, S. A. Grimm, D. Fargo, P. Stojanov, A. Kiezun, G. V. Kryukov, S. L. Carter, G. Saksena, S. Harris, R. R. Shah, M. A. Resnick, G. Getz, D. A. Gordenin, An APOBEC cytidine deaminase mutagenesis pattern is widespread in human cancers. *Nat. Genet.* **45**, 970–976 (2013).
10. L. B. Alexandrov, S. Nik-Zainal, D. C. Wedge, S. A. J. R. Aparicio, S. Behjati, A. V. Biankin, G. R. Bignell, N. Bolli, A. Borg, A.-L. Børresen-Dale, S. Boyault, B. Burkhardt, A. P. Butler, C. Caldas, H. R. Davies, C. Desmedt, R. Eils, J. E. Eyfjörd, J. A. Foekens, M. Greaves, F. Hosoda, B. Hutter, T. Ilicic, S. Imbeaud, M. Imielinsk, N. Jäger, D. T. W. Jones, D. Jones, S. Knappskog, M. Kool, S. R. Lakhani, C. López-Otín, S. Martin, N. C. Munshi, H. Nakamura, P. A. Northcott, M. Pajic, E. Papaemmanuil, A. Paradiso, J. V. Pearson, X. S. Puente, K. Raine, M. Ramakrishna, A. L. Richardson, J. Richter, P. Rosenstiel, M. Schlesner, T. N. Schumacher, P. N. Span, J. W. Teague, Y. Totoki, A. N. J. Tutt, R. Valdés-Mas, M. M. van Buuren, L. van't Veer, A. Vincent-Salomon, N. Waddell, L. R. Yates; Australian Pancreatic Cancer Genome Initiative, ICGC Breast Cancer Consortium, ICGC MMML-Seq Consortium, ICGC PedBrain, J. Zucman-Rossi, P. A. Futreal, U. McDermott, P. Lichter, M. Meyerson, S. M. Grimmond, R. Siebert, E. Campo, T. Shibata, S. M. Pfister, P. J. Campbell, M. R. Stratton, Signatures of mutational processes in human cancer. *Nature* **500**, 415–421 (2013).
11. C. Swanton, N. McGranahan, G. J. Starrett, R. S. Harris, APOBEC enzymes: Mutagenic fuel for cancer evolution and heterogeneity. *Cancer Discov.* **5**, 704–712 (2015).
12. S. A. Roberts, D. A. Gordenin, Hypermutation in human cancer genomes: Footprints and mechanisms. *Nat. Rev. Cancer* **14**, 786–800 (2014).
13. T. Helleday, S. Eshtad, S. Nik-Zainal, Mechanisms underlying mutational signatures in human cancers. *Nat. Rev. Genet.* **15**, 585–598 (2014).
14. M. H. Malim, P. D. Bieniasz, HIV restriction factors and mechanisms of evasion. *Cold Spring Harb. Perspect. Med.* **2**, a006940 (2012).
15. S. Stavrou, S. R. Ross, APOBEC3 proteins in viral immunity. *J. Immunol.* **195**, 4565–4570 (2015).
16. V. Simon, N. Bloch, N. R. Landau, Intrinsic host restrictions to HIV-1 and mechanisms of viral escape. *Nat. Immunol.* **16**, 546–553 (2015).
17. S. Landry, I. Narvaiza, D. C. Linfesty, M. D. Weitzman, APOBEC3A can activate the DNA damage response and cause cell-cycle arrest. *EMBO Rep.* **12**, 444–450 (2011).
18. M. Shinohara, K. Io, K. Shindo, M. Matsui, T. Sakamoto, K. Tada, M. Kobayashi, N. Kadowaki, A. Takaori-Kondo, APOBEC3B can impair genomic stability by inducing base substitutions in genomic DNA in human cells. *Sci. Rep.* **2**, 806 (2012).
19. B. J. M. Taylor, S. Nik-Zainal, Y. L. Wu, L. A. Stebbings, K. Raine, P. J. Campbell, C. Rada, M. R. Stratton, M. S. Neuberger, DNA deaminases induce break-associated mutation showers with implication of APOBEC3B and 3A in breast cancer kataegis. *ELife* **2**, e00534 (2013).
20. B. Mussil, R. Suspène, M.-M. Aynaud, A. Gauvrit, J.-P. Vartanian, S. Wain-Hobson, Human APOBEC3A isoforms translocate to the nucleus and induce DNA double strand breaks leading to cell stress and death. *PLOS One* **8**, e73641 (2013).
21. V. Caval, R. Suspène, M. Shapira, J.-P. Vartanian, S. Wain-Hobson, A prevalent cancer susceptibility APOBEC3A hybrid allele bearing APOBEC3B 3'UTR enhances chromosomal DNA damage. *Nat. Commun.* **5**, 5129 (2014).
22. B. Leonard, J. L. McCann, G. J. Starrett, L. Kosyakovsky, E. M. Luengas, A. M. Molan, M. B. Burns, R. M. McDougle, P. J. Parker, W. L. Brown, R. S. Harris, The PKC/NF-kB signaling pathway induces APOBEC3B expression in multiple human cancers. *Cancer Res.* **75**, 4538–4547 (2015).
23. A. M. Sieuwerts, S. Willis, M. B. Burns, M. P. Look, M. E. Meijer-Van Gelder, A. Schlicker, M. R. Heideman, H. Jacobs, L. Wessels, B. Leyland-Jones, K. P. Gray, J. A. Foekens, R. S. Harris, J. W. M. Martens, Elevated *APOBEC3B* correlates with poor outcomes for estrogen-receptor-positive breast cancers. *Horm. Cancer* **5**, 405–413 (2014).
24. D. W. Cescon, B. Haibe-Kains, T. W. Mak, *APOBEC3B* expression in breast cancer reflects cellular proliferation, while a deletion polymorphism is associated with immune activation. *Proc. Natl. Acad. Sci. U.S.A.* **112**, 2841–2846 (2015).
25. L. R. Yates, M. Gerstung, S. Knappskog, C. Desmedt, G. Gundem, P. Van Loo, T. Aas, L. B. Alexandrov, D. Larsimont, H. Davies, Y. Li, Y. S. Ju, M. Ramakrishna, H. K. Haugland, P. K. Lilleng, S. Nik-Zainal, S. McLaren, A. Butler, S. Martin, D. Glodzik, A. Menzies, K. Raine, J. Hinton, D. Jones, L. J. Mudie, B. Jiang, D. Vincent, A. Greene-Colozzi, P.-Y. Adnet, A. Fatima, M. Maetens, M. Ignatiadis, M. R. Stratton, C. Sotiriou, A. L. Richardson, P. E. Lønning, D. C. Wedge, P. J. Campbell, Subclonal diversification of primary breast cancer revealed by multiregion sequencing. *Nat. Med.* **21**, 751–759 (2015).
26. A. N. Hata, M. J. Niederst, H. L. Archibald, M. Gomez-Caraballo, F. M. Siddiqui, H. E. Mulvey, Y. E. Maruvka, F. Ji, H. E. Bhang, V. Krishnamurthy Radhakrishna, G. Siravegna, H. Hu, S. Raoof, E. Lockerman, A. Kalsy, D. Lee, C. L. Keating, D. A. Ruddy, L. J. Damon, A. S. Crystal, C. Costa, Z. Piotrowska, A. Bardelli, A. J. Iafrate, R. I. Sadreyev, F. Stegmeier, G. Getz, L. V. Sequist, A. C. Faber, J. A. Engelman, Tumor cells can follow distinct evolutionary paths to become resistant to epidermal growth factor receptor inhibition. *Nat. Med.* **22**, 262–269 (2016).
27. K. Kemper, O. Krijgsman, P. Cornelissen-Steijger, A. Shahrabi, F. Weeber, J.-Y. Song, T. Kuilman, D. J. Vis, L. F. Wessels, E. E. Voest, T. N. M. Schumacher, C. U. Blank, D. J. Adams, J. B. Haanen, D. S. Peeper, Intra- and inter-tumor heterogeneity in a vemurafenib-resistant melanoma patient and derived xenografts. *EMBO Mol. Med.* **7**, 1104–1118 (2015).
28. S. Nik-Zainal, H. Davies, J. Staaf, M. Ramakrishna, D. Glodzik, X. Zou, I. Martincorena, L. B. Alexandrov, S. Martin, D. C. Wedge, P. Van Loo, Y. S. Ju, M. Smid, A. B. Brinkman, S. Morganella, M. R. Aure, O. C. Lingjærde, A. Langerød, M. Ringnér, S.-M. Ahn, S. Boyault, J. E. Brock, A. Broeks, A. Butler, C. Desmedt, L. Dirix, S. Dronov, A. Fatima, J. A. Foekens, M. Gerstung, G. K. J. Hooijer, S. J. Jang, D. R. Jones, H.-Y. Kim, T. A. King, S. Krishnamurthy, H.-J. Lee, J. Y. Lee, Y. Li, S. McLaren, A. Menzies, V. Mustonen, S. O'Meara, I. Pauporté, X. Pivot, C. A. Purdie, K. Raine, K. Ramakrishnan, F. G. Rodríguez-González, G. Romieu, A. M. Sieuwerts, P. T. Simpson, R. Shepherd, L. Stebbings, O. A. Stefansson, J. Teague, S. Tommasi, I. Treilleux, G. G. Van den Eynden, P. Vermeulen, A. Vincent-Salomon, L. Yates, C. Caldas, L. van't Veer, A. Tutt, S. Knappskog, B. K. T. Tan, J. Jonkers, Å. Borg, N. T. Ueno, C. Sotiriou, A. Viari, P. A. Futreal, P. J. Campbell, P. N. Span, S. Van Laere, S. R. Lakhani, J. E. Eyfjord, A. M. Thompson, E. Birney, H. G. Stunnenberg, M. J. van de Vijver, J. W. M. Martens, A.-L. Børresen-Dale, A. L. Richardson, G. Kong, G. Thomas, M. R. Stratton, Landscape of somatic mutations in 560 breast cancer whole-genome sequences. *Nature* **534**, 47–54 (2016).
29. D. Juric, P. Castel, M. Griffith, O. L. Griffith, H. H. Won, H. Ellis, S. H. Ebbesen, B. J. Ainscough, A. Ramu, G. Iyer, R. H. Shah, T. Huynh, M. Mino-Kenudson, D. Sgroi, S. Isakoff, A. Thabet, L. Elamine, D. B. Solit, S. W. Lowe, C. Quadt, M. Peters, A. Derti, R. Schegel, A. Huang, E. R. Mardis, M. F. Berger, J. Baselga, M. Scaltriti, Convergent loss of PTEN leads to clinical resistance to a PI(3)Kα inhibitor. *Nature* **518**, 240–244 (2015).
30. S. P. Shah, A. Roth, R. Goya, A. Oloumi, G. Ha, Y. Zhao, G. Turashvili, J. Ding, K. Tse, G. Haffari, A. Bashashati, L. M. Prentice, J. Khattra, A. Burleigh, D. Yap, V. Bernard, A. McPherson, K. Shumansky, A. Crisan, R. Giuliany, A. Heravi-Moussavi, J. Rosner, D. Lai, I. Birol, R. Varhol, A. Tam, N. Dhalla, T. Zeng, K. Ma, S. K. Chan, M. Griffith, A. Moradian, S.-W. G. Cheng, G. B. Morin, P. Watson, K. Gelmon, S. Chia, S.-F. Chin, C. Curtis, O. M. Rueda, P. D. Pharoah, S. Damaraju, J. Mackey, K. Hoon, T. Harkins, V. Tadigotla, M. Sigaroudinia, P. Gascard, T. Tlsty, J. F. Costello, I. M. Meyer, C. J. Eaves, W. W. Wasserman, S. Jones, D. Huntsman, M. Hirst, C. Caldas, M. A. Marra, S. Aparicio, The clonal and mutational evolution spectrum of primary triple-negative breast cancers. *Nature* **486**, 395–399 (2012).
31. S. Nik-Zainal, P. Van Loo, D. C. Wedge, L. B. Alexandrov, C. D. Greenman, K. W. Lau, K. Raine, D. Jones, J. Marshall, M. Ramakrishna, A. Shlien, S. L. Cooke, J. Hinton, A. Menzies, L. A. Stebbings, C. Leroy, M. Jia, R. Rance, L. J. Mudie, S. J. Gamble, P. J. Stephens, S. McLaren, P. S. Tarpey, E. Papaemmanuil, H. R. Davies, I. Varela, D. J. McBride, G. R. Bignell, K. Leung, A. P. Butler, J. W. Teague, S. Martin, G. Jönsson, O. Mariani, S. Boyault, P. Miron, A. Fatima, A. Langerød, S. A. J. R. Aparicio, A. Tutt, A. M. Sieuwerts, Å. Borg, G. Thomas, A. V. Salomon, A. L. Richardson, A.-L. Børresen-Dale, P. A. Futreal, M. R. Stratton, P. J. Campbell, The life history of 21 breast cancers. *Cell* **149**, 994–1007 (2012).
32. E. C. de Bruin, N. McGranahan, R. Mitter, M. Salm, D. C. Wedge, L. Yates, M. Jamal-Hanjani, S. Shafi, N. Murugaesu, A. J. Rowan, E. Grönroos, M. A. Muhammad, S. Horswell,

M. Gerlinger, I. Varela, D. Jones, J. Marshall, T. Voet, P. Van Loo, D. M. Rassl, R. C. Rintoul, S. M. Janes, S.-M. Lee, M. Forster, T. Ahmad, D. Lawrence, M. Falzon, A. Capitanio, T. T. Harkins, C. C. Lee, W. Tom, E. Teefe, S.-C. Chen, S. Begum, A. Rabinowitz, B. Phillimore, B. Spencer-Dene, G. Stamp, Z. Szallasi, N. Matthews, A. Stewart, P. Campbell, C. Swanton, Spatial and temporal diversity in genomic instability processes defines lung cancer evolution. *Science* **346**, 251–256 (2014).

33. A. M. Sieuwerts, M. B. Lyng, M. E. Meijer-van Gelder, V. de Weerd, F. C. Sweep, J. A. Foekens, P. N. Span, J. W. Martens, H. J. Ditzel, Evaluation of the ability of adjuvant tamoxifen-benefit gene signatures to predict outcome of hormone-naive estrogen receptor-positive breast cancer patients treated with tamoxifen in the advanced setting. *Mol. Oncol.* **8**, 1679–1689 (2014).
34. A. V. Lee, S. Oesterreich, N. E. Davidson, MCF-7 cells—Changing the course of breast cancer research and care for 45 years. *J. Natl. Cancer Inst.* **107**, djv073 (2015).
35. Y. H. Ibrahim, S. A. Byron, X. Cui, A. V. Lee, D. Yee, Progesterone receptor-B regulation of insulin-like growth factor—Stimulated cell migration in breast cancer cells via insulin receptor substrate-2. *Mol. Cancer Res.* **6**, 1491–1498 (2008).
36. D. Sachdev, X. Zhang, I. Matise, M. Gaillard-Kelly, D. Yee, The type I insulin-like growth factor receptor regulates cancer metastasis independently of primary tumor growth by promoting invasion and survival. *Oncogene* **29**, 251–262 (2010).
37. J. M. Kidd, T. L. Newman, E. Tuzun, R. Kaul, E. E. Eichler, Population stratification of a common *APOBEC* gene deletion polymorphism. *PLOS Genet.* **3**, e63 (2007).
38. M. Periyasamy, H. Patel, C.-F. Lai, V. T. M. Nguyen, E. Nevedomskaya, A. Harrod, R. Russell, J. Remenyi, A. M. Ochocka, R. S. Thomas, F. Fuller-Pace, B. Győrffy, C. Caldas, N. Navaratnam, J. S. Carroll, W. Zwart, R. C. Coombes, L. Magnani, L. Buluwela, S. Ali, APOBEC3B-mediated cytidine deamination is required for estrogen receptor action in breast cancer. *Cell Rep.* **13**, 108–121 (2015).
39. K. N. Bishop, R. K. Holmes, A. M. Sheehy, N. O. Davidson, S.-J. Cho, M. H. Malim, Cytidine deamination of retroviral DNA by diverse APOBEC proteins. *Curr. Biol.* **14**, 1392–1396 (2004).
40. Q. Yu, D. Chen, R. König, R. Mariani, D. Unutmaz, N. R. Landau, APOBEC3B and APOBEC3C are potent inhibitors of simian immunodeficiency virus replication. *J. Biol. Chem.* **279**, 53379–53386 (2004).
41. B. P. Doehle, A. Schäfer, B. R. Cullen, Human APOBEC3B is a potent inhibitor of HIV-1 infectivity and is resistant to HIV-1 Vif. *Virology* **339**, 281–288 (2005).
42. J. F. Hultquist, J. A. Lengyel, E. W. Refsland, R. S. LaRue, L. Lackey, W. L. Brown, R. S. Harris, Human and rhesus APOBEC3D, APOBEC3F, APOBEC3G, and APOBEC3H demonstrate a conserved capacity to restrict Vif-deficient HIV-1. *J. Virol.* **85**, 11220–11234 (2011).
43. R. Clarke, J. J. Tyson, J. M. Dixon, Endocrine resistance in breast cancer—An overview and update. *Mol. Cell. Endocrinol.* **418**, 220–234 (2015).
44. R. Jeselsohn, G. Buchwalter, C. De Angelis, M. Brown, R. Schiff, *ESR1* mutations—A mechanism for acquired endocrine resistance in breast cancer. *Nat. Rev. Clin. Oncol.* **12**, 573–583 (2015).
45. K. Shi, M. A. Carpenter, K. Kurahashi, R. S. Harris, H. Aihara, Crystal structure of the DNA deaminase APOBEC3B catalytic domain. *J. Biol. Chem.* **290**, 28120–28130 (2015).
46. H. E. Krokan, F. Drabløs, G. Slupphaug, Uracil in DNA—Occurrence, consequences and repair. *Oncogene* **21**, 8935–8948 (2002).
47. J. M. Di Noia, M. S. Neuberger, Molecular mechanisms of antibody somatic hypermutation. *Annu. Rev. Biochem.* **76**, 1–22 (2007).
48. S. Henderson, A. Chakravarthy, X. Su, C. Boshoff, T. R. Fenton, APOBEC-mediated cytosine deamination links *PIK3CA* helical domain mutations to human papillomavirus-driven tumor development. *Cell Rep.* **7**, 1833–1841 (2014).
49. N. McGranahan, C. Swanton, Biological and therapeutic impact of intratumor heterogeneity in cancer evolution. *Cancer Cell* **27**, 15–26 (2015).
50. B. Leonard, S. N. Hart, M. B. Burns, M. A. Carpenter, N. A. Temiz, A. Rathore, R. I. Vogel, J. B. Nikas, E. K. Law, W. L. Brown, Y. Li, Y. Zhang, M. J. Maurer, A. L. Oberg, J. M. Cunningham, V. Shridhar, D. A. Bell, C. April, D. Bentley, M. Bibikova, R. K. Cheetham, J.-B. Fan, R. Grocock, S. Humphray, Z. Kingsbury, J. Peden, J. Chien, E. M. Swisher, L. C. Hartmann, K. R. Kalli, E. L. Goode, H. Sicotte, S. H. Kaufmann, R. S. Harris, APOBEC3B upregulation and genomic mutation patterns in serous ovarian carcinoma. *Cancer Res.* **73**, 7222–7231 (2013).
51. E. W. Refsland, M. D. Stenglein, K. Shindo, J. S. Albin, W. L. Brown, R. S. Harris, Quantitative profiling of the full *APOBEC3* mRNA repertoire in lymphocytes and tissues: Implications for HIV-1 restriction. *Nucleic Acids Res.* **38**, 4274–4284 (2010).
52. M. D. Stenglein, M. B. Burns, M. Li, J. Lengyel, R. S. Harris, APOBEC3 proteins mediate the clearance of foreign DNA from human cells. *Nat. Struct. Mol. Biol.* **17**, 222–229 (2010).
53. C. S. Ross-Innes, R. Stark, A. E. Teschendorff, K. A. Holmes, H. R. Ali, M. J. Dunning, G. D. Brown, O. Gojis, I. O. Ellis, A. R. Green, S. Ali, S.-F. Chin, C. Palmieri, C. Caldas, J. S. Carroll, Differential oestrogen receptor binding is associated with clinical outcome in breast cancer. *Nature* **481**, 389–393 (2012).
54. L. Lackey, E. K. Law, W. L. Brown, R. S. Harris, Subcellular localization of the APOBEC3 proteins during mitosis and implications for genomic DNA deamination. *Cell Cycle* **12**, 762–772 (2013).
55. D. C. Koboldt, Q. Zhang, D. E. Larson, D. Shen, M. D. McLellan, L. Lin, C. A. Miller, E. R. Mardis, L. Ding, R. K. Wilson, VarScan 2: Somatic mutation and copy number alteration discovery in cancer by exome sequencing. *Genome Res.* **22**, 568–576 (2012).

**Acknowledgments:** We thank several laboratory members for thoughtful comments. **Funding:** Animal studies were supported by the Department of Defense Breast Cancer Research Program (BC121347), the Jimmy V Foundation for Cancer Research, and the Prospect Creek Foundation. Additional support for cancer research in the Harris laboratory was provided by the Howard Hughes Medical Institute, Norwegian Centennial Chair Program, and Minnesota Ovarian Cancer Alliance. An NSF Graduate Research Fellowship provided salary support for G.J.S. NIH grant T32 CA009138 provided partial salary support for B.L. Clinical studies were supported by Cancer Genomics Netherlands (A.M.S. and J.W.M.M.), Netherlands Organisation for Scientific Research (NWO) (J.W.M.M.), and European Research Council Advanced Grant no. 322737 (J.A.F.). Statistical analyses were supported by NIH grant P30 CA77598 using the Biostatistics and Bioinformatics Core shared resource of the Masonic Cancer Center, University of Minnesota (R.I.V.). R.S.H. is an investigator of the Howard Hughes Medical Institute. **Author contributions:** R.S.H. and D.Y. designed the xenograft studies. A.M.S., J.A.F., and J.W.M.M. designed the clinical experiments. E.K.L. performed the xenograft experiments with assistance from B.L., whereas G.J.S., N.A.T., and R.I.V. contributed to bioinformatics and statistical analyses. K.L., E.K.L., and A.M.M. performed cell culture studies. M.E.M.-v.G. supplied the clinical data. F.C.G.J.S., P.N.S., J.W.M.M., and J.A.F. provided the clinical samples. A.M.S. quantified gene expression in primary tumors and performed statistical analyses. R.S.H. drafted the manuscript. All authors contributed revisions and approved the submitted version. **Competing interests:** R.S.H. is a cofounder of ApoGen Biotechnologies Inc. D.Y. is a scientific advisory board member of ApoGen Biotechnologies Inc. All other authors declare that they have no competing interests. **Data and materials availability:** All data needed to evaluate the conclusions in the paper are present in the paper and/or the Supplementary Materials. All the reagents and primary data sets reported here are available upon written request to R.S.H.

Submitted 26 July 2016
Accepted 31 August 2016
Published 7 October 2016
10.1126/sciadv.1601737

**Citation:** E. K. Law, A. M. Sieuwerts, K. LaPara, B. Leonard, G. J. Starrett, A. M. Molan, N. A. Temiz, R. I. Vogel, M. E. Meijer-van Gelder, F. C. G. J. Sweep, P. N. Span, J. A. Foekens, J. W. M. Martens, D. Yee, R. S. Harris, The DNA cytosine deaminase APOBEC3B promotes tamoxifen resistance in ER-positive breast cancer. *Sci. Adv.* **2**, e1601737 (2016).

ScienceAdvances
AAAS

# The DNA cytosine deaminase APOBEC3B promotes tamoxifen resistance in ER-positive breast cancer

Emily K. Law, Anieta M. Sieuwerts, Kelly LaPara, Brandon Leonard, Gabriel J. Starrett, Amy M. Molan, Nuri A. Temiz, Rachel Isaksson Vogel, Marion E. Meijer-van Gelder, Fred C. G. J. Sweep, Paul N. Span, John A. Foekens, John W. M. Martens, Douglas Yee and Reuben S. Harris (October 7, 2016)
*Sci Adv* 2016, 2:.
doi: 10.1126/sciadv.1601737